NAVAL POSTGRADUATE SCHOOL
Monterey, California

THESIS

STUDY OF DAMAGE EVOLUTIONS IN COMPOSITE PLATES SUBJECTED TO BENDING LOADS USING MICRO-MACRO ANALYSIS

by

Bruce Howard Hamilton

September 1994

Thesis Advisor: Young Kwon

Approved for public release; distribution is unlimited.

REPORT DOCUMENTATION PAGE

Form Approved
OMB No. 0704-0188

1. AGENCY USE ONLY (Leave Blank)	2. REPORT DATE	3. REPORT TYPE AND DATES COVERED
	September 1994	Master's Thesis

4. TITLE AND SUBTITLE
STUDY OF DAMAGE EVOLUTIONS IN COMPOSITE PLATES SUBJECTED TO BENDING LOADS USING MICRO-MACRO ANALYSIS (U)

5. FUNDING NUMBERS

6. AUTHOR(S)
Hamilton, Bruce Howard

7. PERFORMING ORGANIZATION NAME(S) AND ADDRESS(ES)
Naval Postgraduate School
Monterey, CA 93943-5000

8. PERFORMING ORGANIZATION REPORT NUMBER

9. SPONSORING/ MONITORING AGENCY NAME(S) AND ADDRESS(ES)

10. SPONSORING/ MONITORING AGENCY REPORT NUMBER

11. SUPPLEMENTARY NOTES
The views expressed in this thesis are those of the author and do not reflect the official policy or position of the Department of Defense or the United States Government.

12a. DISTRIBUTION / AVAILABILITY STATEMENT
Approved for public release; distribution is unlimited.

12b. DISTRIBUTION CODE

13. ABSTRACT *(Maximum 200 words)*

The purpose of this study is to develop a computer program that will predict the damage progression in composite plates subjected to bending loads. Kwon's micromechanical model is used to compute the smeared effective moduli from the material properties of fiber and matrix as well as to determine stresses at the constituent level. Failure criteria based on micro-stresses are then applied to determine the extent and type of damage that occur in the composite under various loading conditions. The progression of damage throughout the composite until complete failure of the composite can then be simulated using the current computer program. The numerical prediction for a laminated composite plate containing a hole and subjected to a bending load agrees well with the experimental data.

14. SUBJECT TERMS	15. NUMBER OF PAGES
Composites, Fibrous Laminated Composites, Micromechanical, Finite Element Analysis, Damage Progression	67
	16. PRICE CODE

17. SECURITY CLASSIFICATION OF REPORT	18. SECURITY CLASSIFICATION OF THIS PAGE	19. SECURITY CLASSIFICATION OF ABSTRACT	20. LIMITATION OF ABSTRACT
Unclassified	Unclassified	Unclassified	UL

Approved for public release; distribution is unlimited

STUDY OF DAMAGE EVOLUTIONS IN COMPOSITE PLATES SUBJECTED TO BENDING LOADS USING MICRO-MACRO ANALYSIS

Bruce H. Hamilton
Lieutenant, United States Navy
B.S.Chemistry, Purdue University, 1982
B.S.Chemical Engineering, North Carolina State University, 1986

Submitted in partial fulfillment of the
requirements for the degree of

MASTER OF SCIENCE IN MECHANICAL ENGINEERING

from the

NAVAL POSTGRADUATE SCHOOL
September 1994

Author: 
Bruce H. Hamilton

Approved By: 
Young W. Kwon, Thesis Advisor

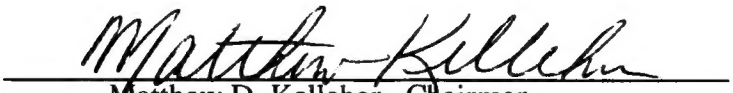
Matthew D. Kelleher, Chairman,
Department of Mechanical Engineering

ABSTRACT

The purpose of this study is to develop a computer program that will predict the damage progression in composite plates subjected to bending loads. Kwon's micromechanical model is used to compute the smeared effective moduli from the material properties of fiber and matrix as well as to determine stresses at the constituent level. Failure criteria based on micro-stresses are then applied to determine the extent and type of damage that occur in the composite under various loading conditions. The progression of damage throughout the composite until complete failure of the composite can then be simulated using the current computer program. The numerical prediction for a laminated composite plate containing a hole and subjected to a bending load agrees well with the experimental data.

TABLE OF CONTENTS

ACKNOWLEDGMENTS

I would like to thank Prof. Kwon for his patients which provide as valuable as his knowledge in the subject matter and Lieutenant Nancy A. Norton, whose unselfish assistance at all times continues to add proof that there is no finer officer than her. Finally, I would like to thank Mr. Dennis Mar for proving that fortran still can be made to serve a useful purpose.

I. INTRODUCTION

Composite materials are becoming more competitive with metallic materials in structural applications. Fiber reinforced composites are the materials of choice when design factors dictate the need for high strength to weight ratio, high stiffness to weight ratio and resistance to harsh environmental conditions. Aircraft and aerospace industries have in particular taken advantage of fiber reinforced composite to decrease weight while maintaining strength. Naval applications of composites are increasingly more common as they have become more of an economically viable option. Most composite structures are usually subjected to bending loads. It is therefore desirable to predict the strengths and failure modes of composite plates subjected to bending loads such that full advantage of the plates' material properties may be used.

Predicting failure mechanisms of composite structures is more difficult than for metallic structures. In addition, most studies dealing with composite failure have been with inplane loading of composite plates. It is the purpose of this study to develope an analytical model to determine the failure modes and strength of laminated fibrous composite plates subjected to bending loads.

Chang and Chang studied failure in a laminated composite plate containing a hole at its center. The plate was subjected to tensile loading. A finite element program was created to model the experimental results. Stress analysis and failure analysis were addressed separately in the program. The computer program modeled stress based on the classical lamination theory of composites. The plate load was increased incrementally so that a progressive damage study of the plate could be performed. As elements failed, their material properties were degraded by the computer program so that failed elements would no longer carry any of the applied load. The elements surrounding failed elements then assumed the load previously supported by the failed elements and experienced increased stress due to those loads. (Chang, 1987)

The failure analysis was based on work done by Yamada and Sun (Yamada, 1978). Matrix cracking, fiber and matrix shearing, and fiber breakage were the identified modes

of failure for the composite constituents. When stresses found in the stress analysis exceed the failure criteria, that element would fail and damage progression in the composite would be computed. The computer model developed by Chang and Chang was determined to provide an accurate predication of composite damage propagation. (Chang, 1987)

Owen and Li stated that for composite plates a macromechanical approach involving the use of the classical laminated plate theory was not sufficiently accurate for stress calculations, yet a micro approach would be too numerically cumbersome to provide any results. Laminated composite plates have been shown to have the greater effect of transverse shear deformation as the plate thickness increases relative to the plate length and as such the classical laminated plate theory is not sufficiently accurate to model orthotropic and anisotropic laminates. Owen and Li used a model based on inplane displacements across the plate thickness, in which inplane displacements are pieces-wise linear and lateral displacements constant across the thickness. This allowed for the three dimensional model to be reduced to a two dimensional plate bending model. (Owen, 1987)

Kwon's use of micromechanical analysis provides the means to determine damage progression at the constituent level for laminated fibrous composites. The micromechanical model is used to determine smeared composite properties from the fiber and matrix material properties. Macro analysis is then used to determine displacements and strains of composite using the smeared composite properties in the finite element analysis. Microstresses are determined for each composite constituent in the element by using the micromechanical model in conduction with the composite strains. Failure analysis can then be applied at the fiber and matrix level. Damage progression of the composite may be predicted based on the strengths and failure modes of the fibers and matrix that comprise the laminated composite. (Kwon, 1993)

II. MICROMECHANICAL MODEL

A. OVERVIEW

The investigation of damage progression in a laminated fibrous composite plate is undertaken using a micromechanical model. Kwon's micromechanical model permits the calculation of microstresses for a composite using the material properties of the fiber and matrix that make up that composite (Kwon, 1993). The microstresses are evaluated with a set of failure criteria, and thus a study of damage throughout the composite with details of fiber and matrix damages is possible. The mircromechanical model also computes the smeared composite material properties from the fiber and matrix material properties.

B. MICROMECHANICAL CELL

The micromechanical unit cell is made of a fiber and surrounding matrix material. Using the symmetry of the cell, only a quarter of the actual cell needs to be modelled as shown in Figure 1. The fiber direction is taken as the direction along the 1 axis. The cell is

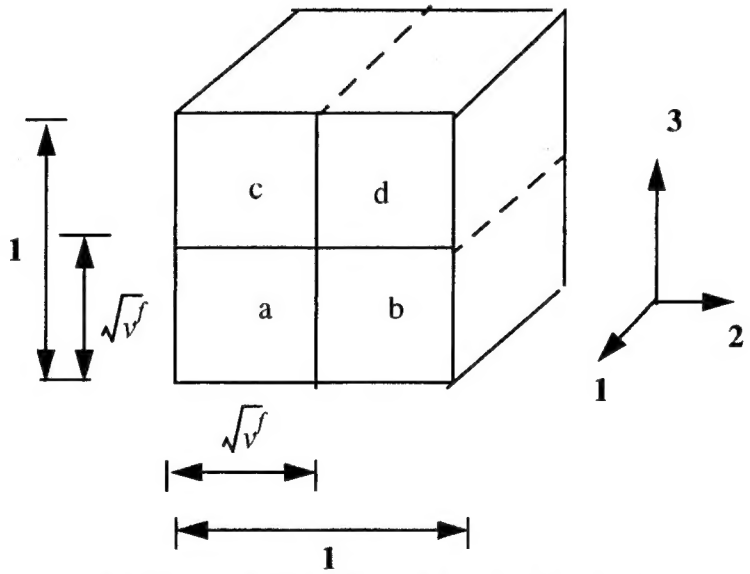

Figure 1. Kwon's Unit Cell and Subcells

divided into four subcells. Each subcell size depends on the volume fraction of the fiber, v_f. (Kwon, 1993)

The stresses, $\bar{\sigma}_{ij}$, and strains, $\bar{\varepsilon}_{ij}$, of the composite, are the volume average of the subcell stresses, σ^{α}_{ij}, and subcell strains, $\varepsilon^{\alpha}_{ij}$, as given below (Kwon, 1993):

$$\bar{\sigma}_{ij} = v^f \sigma^a + v^f\left(1-\sqrt{v^f}\right)\sigma^b{}_{ij} + v^f\left(1-\sqrt{v^f}\right)\sigma_{ij}{}^c + \left(1-\sqrt{v^f}\right)^2 \sigma_{ij}{}^d \qquad \text{Eq 1}$$

$$\bar{\varepsilon}_{ij} = v^f \varepsilon^a + v^f\left(1-\sqrt{v^f}\right)\varepsilon^b{}_{ij} + v^f\left(1-\sqrt{v^f}\right)\varepsilon_{ij}{}^c + \left(1-\sqrt{v^f}\right)^2 \varepsilon_{ij}{}^d \qquad \text{Eq 2}$$

where a is the fiber subcell, b, c, and d are the matrix subcells.

Stress continuity at subcell interfaces is satisfied by the following relationships (Kwon, 1993):

$$\sigma^a{}_{22} = \sigma^b{}_{22}, \sigma^c{}_{22} = \sigma^d{}_{22}, \sigma^a{}_{33} = \sigma^c{}_{33}, \sigma^b_{33} = \sigma^d_{33} \qquad \text{Eq 3}$$

$$\sigma^a{}_{12} = \sigma^b{}_{12}, \sigma^c{}_{12} = \sigma^d{}_{12}, \sigma^a{}_{13} = \sigma^c{}_{13}, \sigma^b_{13} = \sigma^d_{13} \qquad \text{Eq 4}$$
$$\sigma^a{}_{23} = \sigma^b{}_{23} = \sigma^c{}_{22} = \sigma^d{}_{23}$$

The strains of the subcells are assumed to meet the following requirements (Kwon, 1993):

$$\varepsilon^a{}_{11} = \varepsilon^b{}_{11} = \varepsilon^c{}_{11} = \varepsilon^d{}_{11} \qquad \text{Eq 5}$$
$$\varepsilon^a{}_{22} + \varepsilon^b{}_{22} = \varepsilon^c{}_{22} + \varepsilon^d{}_{22}$$
$$\varepsilon^a{}_{33} + \varepsilon^c{}_{33} = \varepsilon^b{}_{33} + \varepsilon^d{}_{33}$$

$$\varepsilon^a{}_{12} + \varepsilon^b{}_{12} = \varepsilon^c{}_{12} + \varepsilon^d{}_{12} \qquad \text{Eq 6}$$
$$\varepsilon^a{}_{13} + \varepsilon^c{}_{13} = \varepsilon^b{}_{13} + \varepsilon^d{}_{13}$$

The constitutive equation for each subcell based on Hooke's law is given by:

$$\sigma^{\alpha}{}_{ij} = E^{\alpha}{}_{ijkl}\varepsilon^{\alpha}{}_{kl} \qquad \text{Eq 7}$$

where i, j = 1, 2, 3 and α = a, b, c, d.

The stress for each subcell expressed in Equation 7 is substituted into Equation 3 and Equation 4 to have an expression for stress continuity represented in terms of subcell

strains. The resultant equations along with Equation 2, Equation 5 and Equation 6 are solved simultaneously to result in subcells strains given by average composite strains. Subcell strains expressed in terms of the average composite strains are substituted into Equation 7 and the resultant subcell stresses expressed in terms of the composite strains are plugged into Equation 1 to result in the relationship between the composite stresses and composite strains. This relationship gives the smeared composite material properties expressed in terms of the fiber and matrix material properties. (Kwon, 1993)

As a result, the micromechanical model computes the composite material properties using the constitutive fiber and matrix material properties. In addition, the model gives the relationship between microstresses (and strains) and composite stresses (and strains). That is, microstrains are found from composite strains. The microstrains are then used with Hooke's law for each constituent to determine the microstresses, from which the composite stresses are determined.

III. FINITE ELEMENT MODEL

A. PLATES IN BENDING

One objective of this study is to develope a computer program that will model the failure experienced by a thin composite plate due to a bending load. The finite element method along with Kwon's micromechanical model is used for the present study. The plate bending element used in this study is described below.

A plate bending element is shown in Figure 2 where x, y, and z describe the global

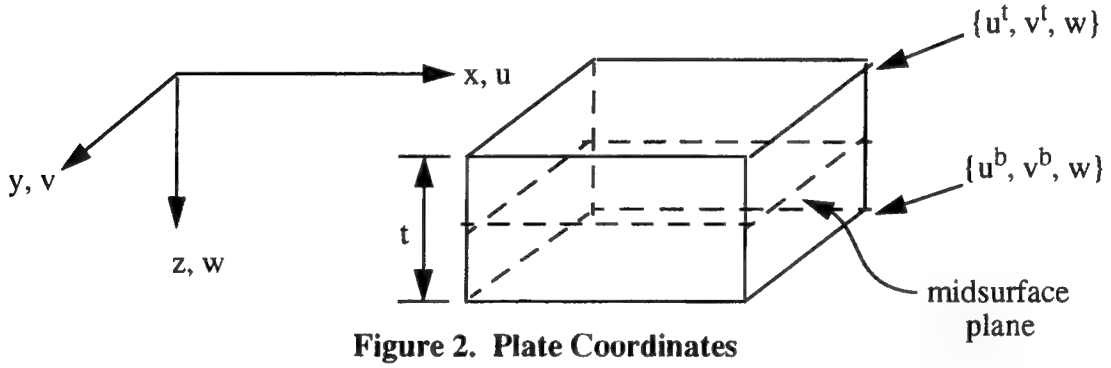

Figure 2. Plate Coordinates

coordinates of points of the plate and u, v, and w are the displacements of those points. t is the plate thickness. The xy plane is parallel to the midsurface plane prior to deflection.

The displacement of any point in the plate can be expressed as (Ugural, 1987).

$$\{d\}_e = \{u(x,y,z), v((x,y,z), w(x,y))\}^T \qquad \text{Eq 8}$$

That is, the inplane displacements vary through the plate thickness while the transverse displacement remains constant through the plate thickness. This displacement within the element may be written in terms of shape functions and nodal displacement.

$$\{d\}_e = \sum_i^n N_i \{\delta\}_i \qquad \text{Eq 9}$$

Equation 9 can be rewritten in a matrix form as given below (Owen, 1987),

$$\{d\}_e = [N]\{\delta\}_e \qquad \text{Eq 10}$$

where $\{\delta\}_e$ is the nodal displacement vector for a plate element. $\{\delta\}_i$ is the nodal displacements for the i^{th} node of an element.

$$\{\delta\}_i = \begin{Bmatrix} u_i^b \\ v_i^b \\ u_i^t \\ v_i^t \\ w_i \end{Bmatrix} \qquad \text{Eq 11}$$

where superscripts b and t denote the inplane displacements at the bottom and top sides of the plate element, respectively. A four node quadrilateral element is used for the present study for interpolation of displacements in the x-y plane as shown in Figure 3:

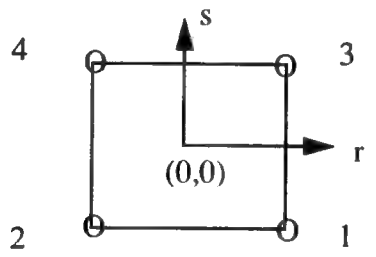

Figure 3. Quadrilateral Element

The shape function for the quadrilateral element is given in terms of the natural coordinate system:

$$N_i = \frac{1}{4}(1 + rr_i)\ (1 + ss_i) \qquad \text{Eq 12}$$

where i= 1,2,3,4, and r_i and s_i are the local coordinates of the corners of the quadrilateral element whose values are either -1 or +1.

Linear shape functions are given below in terms of the third natural coordinate axis, which is mapped into the plate thickness direction in the physical coordinate system:

$$H_1(q) = \frac{1}{2}(1-q)$$
$$H_2(q) = \frac{1}{2}(1+q) \qquad \text{Eq 13}$$

Combining the previous bilinear shape functions, Equation 12 with the linear shape functions, Equation 13, yields (Kwon, 1988):

$$\bar{N}_{2j-1} = N_j(r,s)\,H_1(q)$$
$$\bar{N}_{2j} = N_j(r,s)\,H_2(q) \qquad j = 1, 2, 3, 4 \qquad \text{Eq 14}$$

Three cartesian displacements within a plate element are then written as:

$$u_e = \bar{N}_1 u^b{}_1 + \bar{N}_2 u^t{}_1 + \bar{N}_3 u^b{}_2 + \bar{N}_4 u^t{}_2 + \bar{N}_5 u^b{}_3 + \bar{N}_6 u^t{}_3 + \bar{N}_7 u^b{}_4 + \bar{N}_8 u^t{}_4$$
$$v_e = \bar{N}_1 v^b{}_1 + \bar{N}_2 v^t{}_1 + \bar{N}_3 v^b{}_2 + \bar{N}_4 v^t_2 + \bar{N}_5 v^b{}_3 + \bar{N}_6 v^t{}_3 + \bar{N}_7 v^b{}_4 + \bar{N}_8 v^t{}_4 \qquad \text{Eq 15}$$
$$w_e = N_1 w_1 + N_2 w_2 + N_3 w_3 + N_4 w_4$$

where u and v are inplane displacements and w is the transverse displacement. Subscript and superscript for the nodal displacements indicate the node number, and top or bottom plane displacement of the plate, respectively. Since there is no rotational degree of freedom in the present plate bending element, the inplane displacements have two components at one nodal point: i.e. top plane displacement and bottom plane displacement.

When a bending load is applied to a plate to cause it to deflect from its original configuration, deflection, stresses and strains associated with the deformation will follow several basic assumptions. These assumptions are (Ugural, 1987):

1) The normal stress to the midsurface, σ_z, is negligible
2) Deflection of the plate is small in comparison with the thickness of the plate
3) The normal strain in the plate thickness direction, ε_z may be neglected.

Strains for the element are in a matrix form:

$$\begin{Bmatrix} \varepsilon_x \\ \varepsilon_y \\ \gamma_{xy} \\ \gamma_{xz} \\ \gamma_{yz} \end{Bmatrix}_e = \begin{bmatrix} \frac{\partial}{\partial x} & 0 & 0 \\ 0 & \frac{\partial}{\partial y} & 0 \\ \frac{\partial}{\partial y} & \frac{\partial}{\partial x} & 0 \\ \frac{\partial}{\partial z} & 0 & \frac{\partial}{\partial x} \\ 0 & \frac{\partial}{\partial z} & \frac{\partial}{\partial y} \end{bmatrix} \begin{Bmatrix} u \\ v \\ w \end{Bmatrix}_e \qquad \text{Eq 16}$$

Equation 10 is used to represent the displacements in Equation 16 so that strains can be expressed in terms of the shape functions and displacements. Elemental strain in terms of shape functions and displacements are shown in the Appendix. The matrix of shape function derivatives is referred to as [B]. Strain equations may be expressed as:

$$\{\varepsilon\}_e = [B]\{\delta\}_e \qquad \text{Eq 17}$$

Stresses of a plate in accordance with the assumptions listed for this study are:

$$\{\sigma\} = \begin{Bmatrix} \sigma_x \\ \sigma_y \\ \tau_{xy} \\ t_{xz} \\ \tau_{yz} \end{Bmatrix} \qquad \text{Eq 18}$$

Stresses are obtained from the strains using Hooke's law. For an isotropic homogenous plate, stresses are (Ugural, 1987):

$$\begin{Bmatrix} \sigma_x \\ \sigma_y \\ \tau_{xy} \\ t_{xz} \\ \tau_{yz} \end{Bmatrix}_e = \begin{bmatrix} \frac{E}{1-\nu^2} & \frac{E\nu}{1-\nu^2} & 0 & 0 & 0 \\ \frac{E\nu}{1-\nu^2} & \frac{E}{1-\nu^2} & 0 & 0 & 0 \\ 0 & 0 & \frac{E}{2(1+\nu)} & 0 & 0 \\ 0 & 0 & 0 & \frac{E}{2(1+\nu)} & 0 \\ 0 & 0 & 0 & 0 & \frac{E}{2(1+\nu)} \end{bmatrix} \begin{Bmatrix} \varepsilon_x \\ \varepsilon_y \\ \gamma_{xy} \\ \gamma_{xz} \\ \gamma_{yz} \end{Bmatrix} \quad \text{Eq 19}$$

where E is the elastic modulus and ν is poisson's ratio.

The matrix of material properties may be written in a more condensed form and called [D]. This allows Equation 19 to be written as:

$$\{\sigma\}_e = [D]\{\varepsilon\}_e \quad \text{Eq 20}$$

For a unidirectional fibrous composite, the [D] matrix is:

$$[D] = \begin{bmatrix} D_{11} & D_{12} & 0 & 0 & 0 \\ D_{12} & D_{22} & 0 & 0 & 0 \\ 0 & 0 & D_{33} & 0 & 0 \\ 0 & 0 & 0 & D_{44} & 0 \\ 0 & 0 & 0 & 0 & D_{55} \end{bmatrix} \quad \text{Eq 21}$$

$$D_{11} = \frac{E_{11}}{1-\mu_{12}\mu_{21}}$$

$$D_{12} = \frac{E_{11}\mu_{21}}{1-\mu_{12}\mu_{21}}$$

$$D_{22} = \frac{E_{22}}{1-\mu_{12}\mu_{21}} \quad \text{Eq 22}$$

$$D_{33} = G_{12}$$

$$D_{44} = G_{13}$$

$$D_{55} = G_{23}$$

in which E_{11} is Young's modulus in the direction of the 1 axis as shown in Figure 1, E_{22} is modulus along the 2 axis, μ_{12} is poisson's ratio on the 1 face in the 2 direction, μ_{21} is possion's ratio on the 2 face in the 1 direction, and G_{ij} is the shear modulus associated with i and j axes.

Equation 20 shows that stresses are obtained from strains and those strains are determined using displacements in Equation 17. A method now must be developed to determine displacements such that stress can be obtained. Energy methods can be used to find displacements. The Rayleigh-Ritz method is particular suited to determining unknown displacements. The procedure of using the Rayleigh-Ritz method is (Ugural, 1987):

1) Assume a displacemnet function in terms of unknown nodal parameters
2) Compute the potential energy, Π, in terms of the unknown parameters which describe the total work, W, and strain energy, U

$$\Pi = U - W \qquad \text{Eq 23}$$

3) Apply the principle of minimum potential energy and solve for the displacements.

Strain energy, U, may be expressed in terms of stress and stain (Ugural, 1987).

$$U = \frac{1}{2}\int_V (\sigma_x\varepsilon_x + \sigma_y\varepsilon_y + \sigma_z\varepsilon_z + \tau_{xy}\gamma_{xy} + \tau_{yz}\gamma_{xy} + \tau_{yz}\gamma_{yz})\, dV \qquad \text{Eq 24}$$

where V is the volume of the body.

The work, W, done by external forces, F (per unit volume), and surface forces, T (per unit area) is given by (Ugural, 1987):

$$W = \int_V (F_x u + F_y v + F_z w)\, dV + \int_A (T_x u + T_y v + T_z w)\, dS \qquad \text{Eq 25}$$

where A is the boundary surface of the body.

Using the principle of minimum potential energy, Π is minimized such that (Ugural, 1987):

$$\delta\Pi = \delta\left[\frac{1}{2}\int_V (\sigma_x\varepsilon_x + \sigma_y\varepsilon_y + \sigma_z\varepsilon_z + \tau_{xy}\gamma_{xy} + \tau_{yz}\gamma_{xy} + \tau_{yz}\gamma_{yz})\, dV \right. \qquad \text{Eq 26}$$
$$\left. -\left(\int_V (F_x u + F_y v + F_z w)\, dV + \int_A (T_x u + T_y v + T_z w)\, dS\right)\right] = 0$$

The potential energy equation can be written using the finite element discretization

$$\Pi = \sum \int_{V_e} \left(\frac{1}{2} \{\varepsilon\}_e^T \{\sigma\}_e - \{d\}_e^T \{F\}_e \right) dV - \sum \int_{S_e} \{d\}_e^T \{T\}_e dS \quad \text{Eq 27}$$

where summations are over the discretized finite elements, and {d} is the displacement vector. Stresses in Equation 27 can be written in terms of strains and [D] from Equation 20.

$$\Pi = \sum_1 \int_V \left(\frac{1}{2} \{\varepsilon\}_e^T [D] \{\varepsilon\}_e - \{d\}^T{}_e \{F\}_e \right) (dV) \quad \text{Eq 28}$$
$$- \sum_1 \int_S \{d\}_e^T \{T\}_e dS$$

Displacements for each element are represented by the unknown nodal displacements $\{\delta\}_i$, and shape functions. Strains can now be expressed in terms of elemental nodal displacements and derivatives of the shape functions (Owen, 1987). Using Equation 17 for the strain in terms of the [B] matrix and nodal displacements, and Equation 10 for the displacement function, Equation 28 becomes:

$$\Pi = \sum \int_{V_e} \left(\frac{1}{2} \{\delta\}_e^T [B]^T [D] [B] \{\delta\}_e - \{\delta\}^T [N]^T \{F\}_e \right) dV \quad \text{Eq 29}$$
$$- \sum \int_{S_e} \{\delta\}^T [N]^T \{T\}_e dS$$

After minimizing the total potential energy with respect to the nodal displacements, the element stiffness matrix is defined as (Owen, 1987):

$$[k]_e = \int_{V_e} [B]^T [D] [B] \, dV \quad \text{Eq 30}$$

The element force matrix is formed by combining the work done by external surface forces and body forces:

$$\{Q\}_e = \int_{V_e} [N]^T \{F\} \, dV + \int_A [N]^T \{T\} \, dS: \quad \text{Eq 31}$$

Assembling all element matrices and vectors, the system equation is:

$$[K] \{\delta\} = \{Q\} \quad \text{Eq 32}$$

The unknown nodal displacement can thus be determined.

Since the shape of the elements can be irregular quadrilateral, domain and boundary integrations of such shapes are solved using the natural coordinate system (r, s, q) (Segerlind, 1984). This integration must be done numerically and will use the Gauss-Legendre integration technique. Since the natural coordinate system is used for numerical integration to compute the integral, the Jacobian matrix, [J], must be used for mapping between the physical and natural coordinate systems, that is,

$$[J] = \begin{bmatrix} \frac{\partial x}{\partial r} & \frac{\partial y}{\partial r} & \frac{\partial z}{\partial r} \\ \frac{\partial x}{\partial s} & \frac{\partial y}{\partial s} & \frac{\partial z}{\partial s} \\ \frac{\partial x}{\partial q} & \frac{\partial y}{\partial q} & \frac{\partial z}{\partial q} \end{bmatrix} \qquad \text{Eq 33}$$

The stiffness matrix can now be represented in terms of the natural coordinate system (Segerlind, 1984).

$$[k]_e = \int_{V_e} [B]^T [D] [B] \, dV = \int_{-1}^{1}\int_{-1}^{1}\int_{-1}^{1} [B]^T [D] [B] |J| \, dr\,ds\,dq \qquad \text{Eq 34}$$

The integrals for the natural coordinate system are defined on the interval +1 to -1. Using numerical integration with n, m, l integration points along each direction, the stiffness matrix becomes:

$$[k]_e = \int_V [B]^T [D] [B] \, dV = \sum_{i=1}^{m}\sum_{j=1}^{n}\sum_{k=1}^{l} W_i W_j W_k \Big([B]^T [D] [B] |J| \Big)_{ijk}$$

where $()_{ijk}$ indicates the function is evaluated at (r_i, s_j, q_k). That is, [B], [D], and |J| are evaluated at their sampling points and W is the weight coefficients for Gauss quadrature (Segerlind, 1984).

With the calculation of a stiffness matrix and a force vector, displacements for the nodal points of the plate can be determined. These displacements are used with Equation 17 to solve for the strain. Once the strains are determined, microstrains, microstresses and

macrostresses are determined using the micromechanical model described in the previous chapter.

IV. MICRO-MACRO ANALYSIS

A. MICRO-MACRO ANALYSIS

To find the damage progress in a plate due to an external loading, a micro-macromechanical approach is used. Kwon's micromechanical model is the basis for the procedure. Composite material properties are determined from the fiber and matrix material properties using the micromechanical model. These composite properties are then used to determine nodal displacements from the finite element analysis (macro analysis). Equation 17 shows that macro-strains are obtained from displacements. The micromechanical model is again used with the macro-strains to derive the micro-strains of each element. Micro-stresses are calculated using micro-strains. Failure criteria applied to measure damage progression in the composite.

[B] can be decomposed into two parts; $[B]_b$ for the bending strains and $[B]_s$ for the shear stains (Kwon, 1994).

$$[B]_b = \begin{bmatrix} \frac{\partial u}{\partial x} \\ \frac{\partial v}{\partial y} \\ \frac{\partial u}{\partial y} + \frac{\partial v}{\partial x} \end{bmatrix} \qquad \text{Eq 35}$$

$$[B]_{shear\,(i)} = \begin{bmatrix} \frac{\partial u}{\partial z} + \frac{\partial w}{\partial x} \\ \frac{\delta v}{\delta z} + \frac{\delta w}{\delta y} \end{bmatrix} \qquad \text{Eq 36}$$

$[B]_b$ is evaluated at four integration points in the rs plane while $[B]_s$ is evaluated at one integration point to prevent shear locking. As a result, the bending strains are averaged to produce one value for each element in the same manner as the transverse shear strains.

B. FAILURE CRITERIA

In order to study the damage progression in a composite subjected to a bending load, the following failure criteria are used (Berner, 1993):

$$\left|\sigma_{11}{}^{f}\right| \geq \begin{cases} X_t^{\,f} \; if \; \sigma_{11} > 0 \\ X_c^{\,f} \; if \; \sigma_{11} < 0 \end{cases} \qquad \text{Eq 37}$$

$$\left(\frac{\sigma_{22}{}^{m}}{X^{m}{}_{t}}\right)^2 + \left(\frac{\sigma_{12}{}^{m}}{S^{m}}\right)^2 \geq 1 \text{ if } \sigma^{m}{}_{22} > 0$$

$$\left(\frac{\sigma_{22}{}^{m}}{X^{m}{}_{t}}\right)^2 + \left(\frac{\sigma_{12}{}^{m}}{S^{m}}\right)^2 \geq 1 \text{ if } \sigma^{m}{}_{22} < 0 \qquad \text{Eq 38}$$

in which $\sigma^{f}{}_{11}$ is the longitudinal fiber stress and X^{f} is the ultimate strength of the fiber in the longitudinal direction. Subscripts t and c denote tensile and compressive strengths. $\sigma^{m}{}_{22}$ is the transverse matrix stress, X^{m} is the ultimate strength of the matrix, $\sigma^{m}{}_{12}$ is the matrix shear stress, and S_m is the ultimate shear strength of the matrix.

The failure criteria are used in determining the failure of the composite in four different modes; fiber failure in compression or tension and matrix failure in compression or tension. If any of these failure modes occurs, then the material properties for the fiber and/or matrix related to the failure are degraded at the failed location. This degradation of material properties in the computer modeling is accomplished by multiplying those material properties by 0.005, effectively reducing the properties to small values but non-zero values allowing the material property matrices to be non-singular. For subsequent calculations, those failed fiber and/or matrix will not take any of the applied load. (Since the failed material properties are not exactly zeros, the failed location may still carry very small insignificant loads.)

The load is applied incrementally. An initial load is chosen and applied to the composite. The computer program checks whether computed stresses satisfy the failure

criteria. If there is no failure of either the fiber or matrix in the composite, the program increases the load incrementally as directed by the input file until some type of failure occurs or the maximum prescribe load is applied.

If some type of failure has occurred, then that fiber and/or matrix material is degraded as described previously. Another iteration will now be carried out using this "damaged" element(s). Each loading condition is allow to run through only five iterations. This is done to more closely model actual loading of the plate by a testing machine that continually increases the load over a finite period of time. The failure of the composite itself was based on the degree and direction of the failure for the fibers and matrix.

The failure is checked at the numerical integration points of each plate bending element. The elemental stiffness matrix is the sum of stiffness matrices for bending and shear (Kwon, 1994).

$$[k]_e = [k]_b + [k]_s \qquad \text{Eq 39}$$

For the bending stiffness, 2-point integration rule is used in every direction. However, 1-point integration rule is used for the shear stiffness on the inplane directions and 2-point rules on the thickness direction. As a result, the stresses due to bending are computed at four points in the plane of a plate element while the transverse shear stresses at one point. The bending stresses are averaged for four points on both tension and compression sides of a plate element. Finally the averaged bending stresses and the shear stresses are used for the failure criteria to represent failure of the element either on the tension or compressive side.

V. RESULTS

A. PLATE WITH A HOLE SUBJECTED TO UNIFORM BENDING

A numerical prediction was conducted using the present micro-macro damage model for the laminated composite used by Yang in his experimental testing. The laminated composite plate was a carbon/epoxy composite (IM6/3501-6) manufactured by Hercules Materials Company of Magna, Utah. The fibers were in aligned in the 0^0 direction. Yang used a 12 inch by 1 inch plate containing a 0.250 inch diameter hole at the center and subjected to a four point bending test to create an uniform bending moment along the edge of the plate. (Yang, 1994)

The material properties of the composite used in the bending study were determined from experiments. (See Table 1)

Property	Fiber	Matrix
Elastic Modulus(Msi)	2.30	0.200
Poisson's Ratio	0.270	0.360
Fiber volume fraction	0.250	N/A

Table 1. Material Properties of Composite

Yang showed that for the one-quarter symmetric sample of the plate, as in Figure 4, the failure loading corresponded to 230 lb-in applied moment.

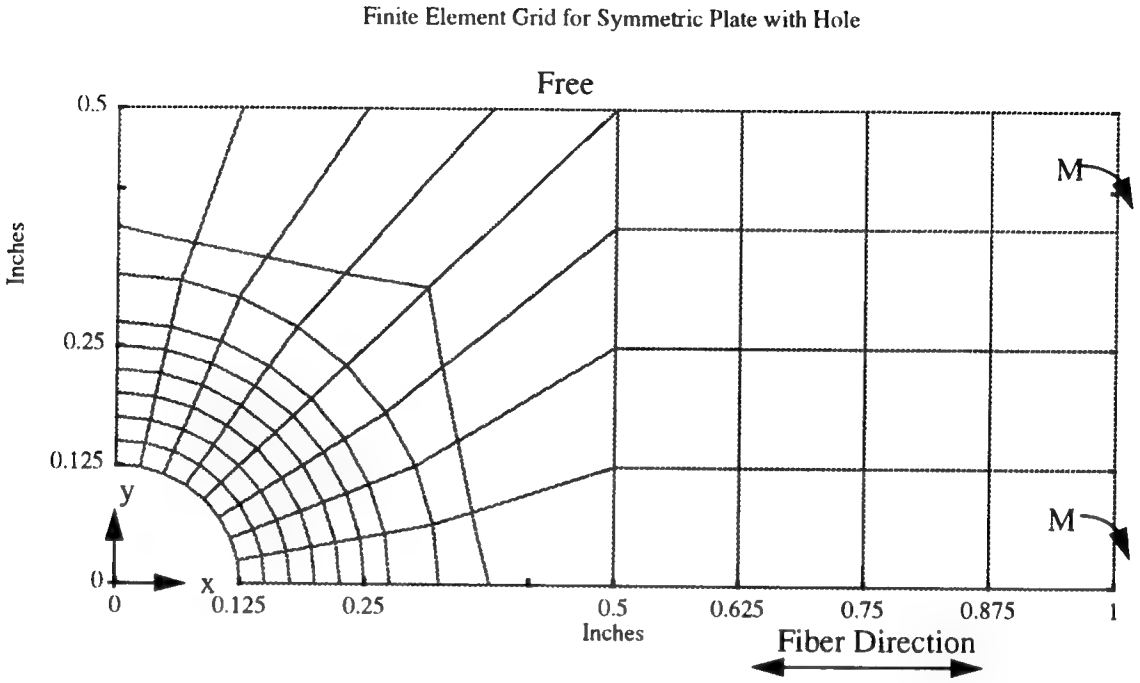

Figure 4. Symmetric Plate with Hole

Failure of each element of the plate is based on the criteria of Equation 37 and Equation 38. Total failure of the composite is determined from when there is nearly complete failure of the fibers along the y-axis. Matrix failure occurs in different forms. Matrix may fail along the y-axis creating a matrix cracking and/or it can fail along the x-axis to cause fiber splitting. The underlying definition of composite failure in this case is the inability of the composite to carry an applied load. The damage progression predicted using the present micro-macro model is plotted in Figure 5 through Figure 8. As seen in Figure 5 and Figure 6, matrix cracking occurs along the fiber direction causing fiber splitting. As the load increases, fiber breakage occurs along the minimum section of the plate until the final fracture at 200 lb-in the failure modes agree with the experimental observation and the final failure load is 15% less than the experimental failure load.

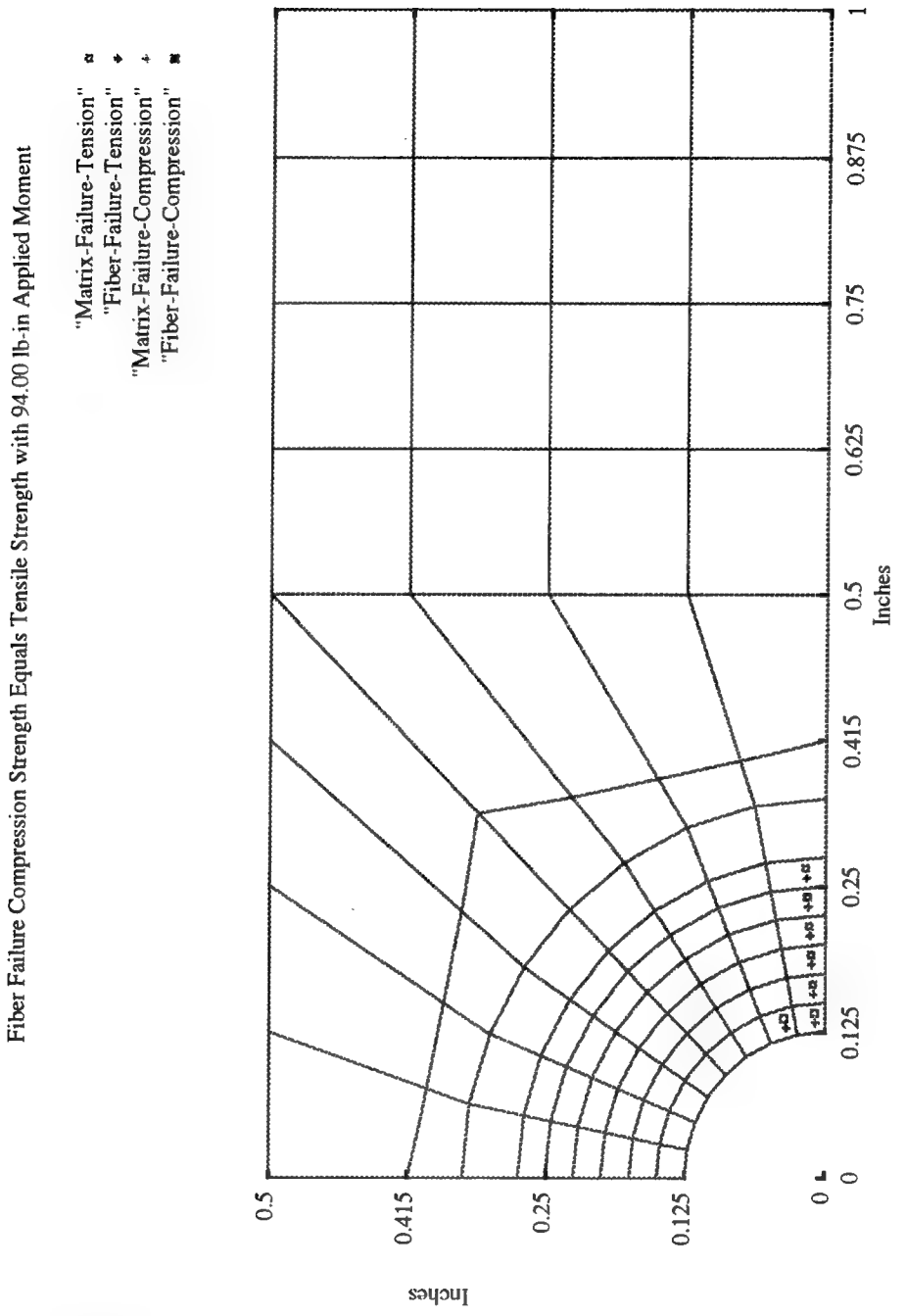

Figure 5. Fiber Failure Compression Strength Equal to Tensile Strength with 94.00 lb-in Applied Moment

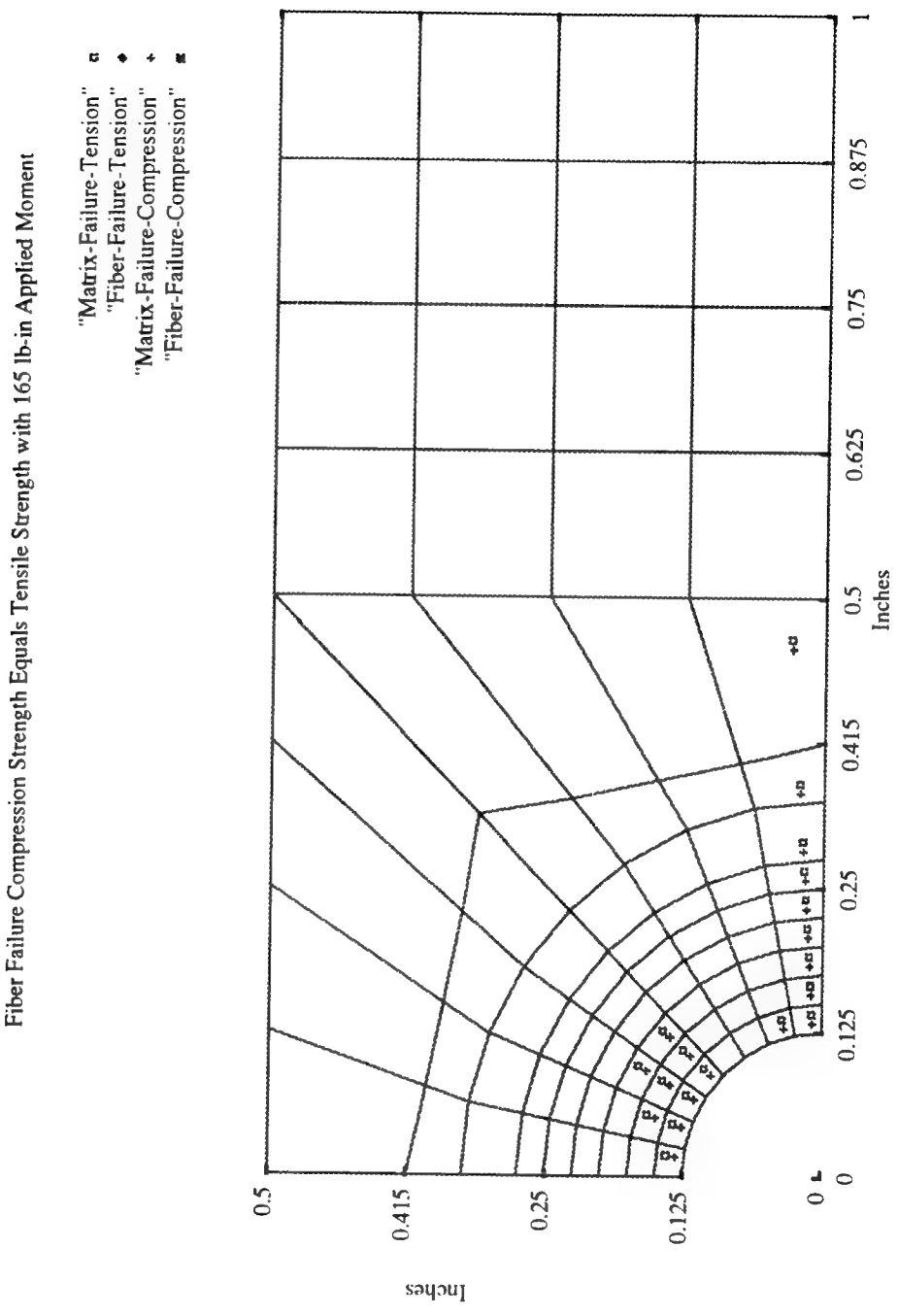

Figure 6. Fiber Failure Compression Strength Equal to Tensile Strength with 165 lb-in Applied Moment

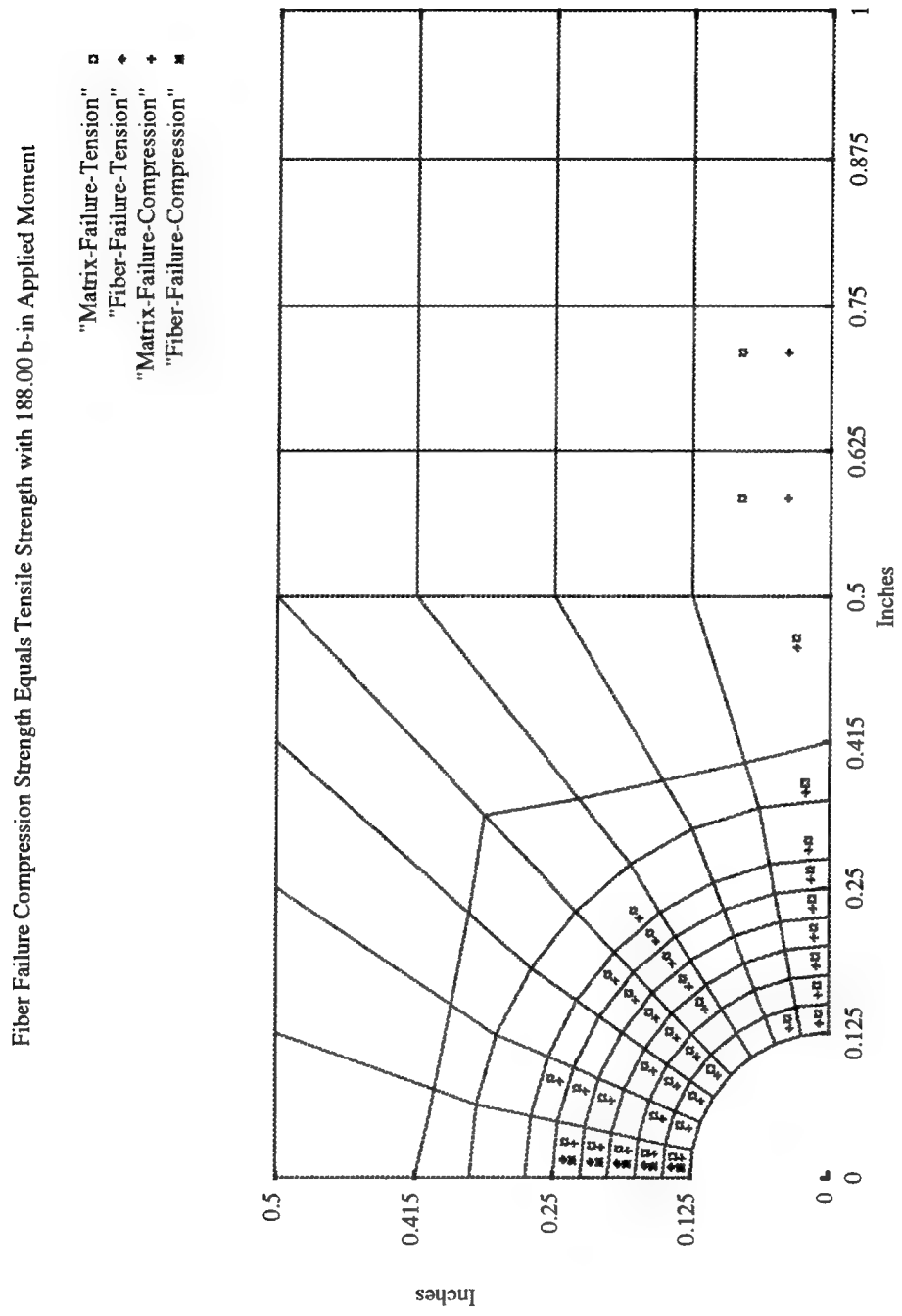

Figure 7. Fiber Failure Compression Strength Equal to Tensile Strength with 188.00 lb-in Applied Moment

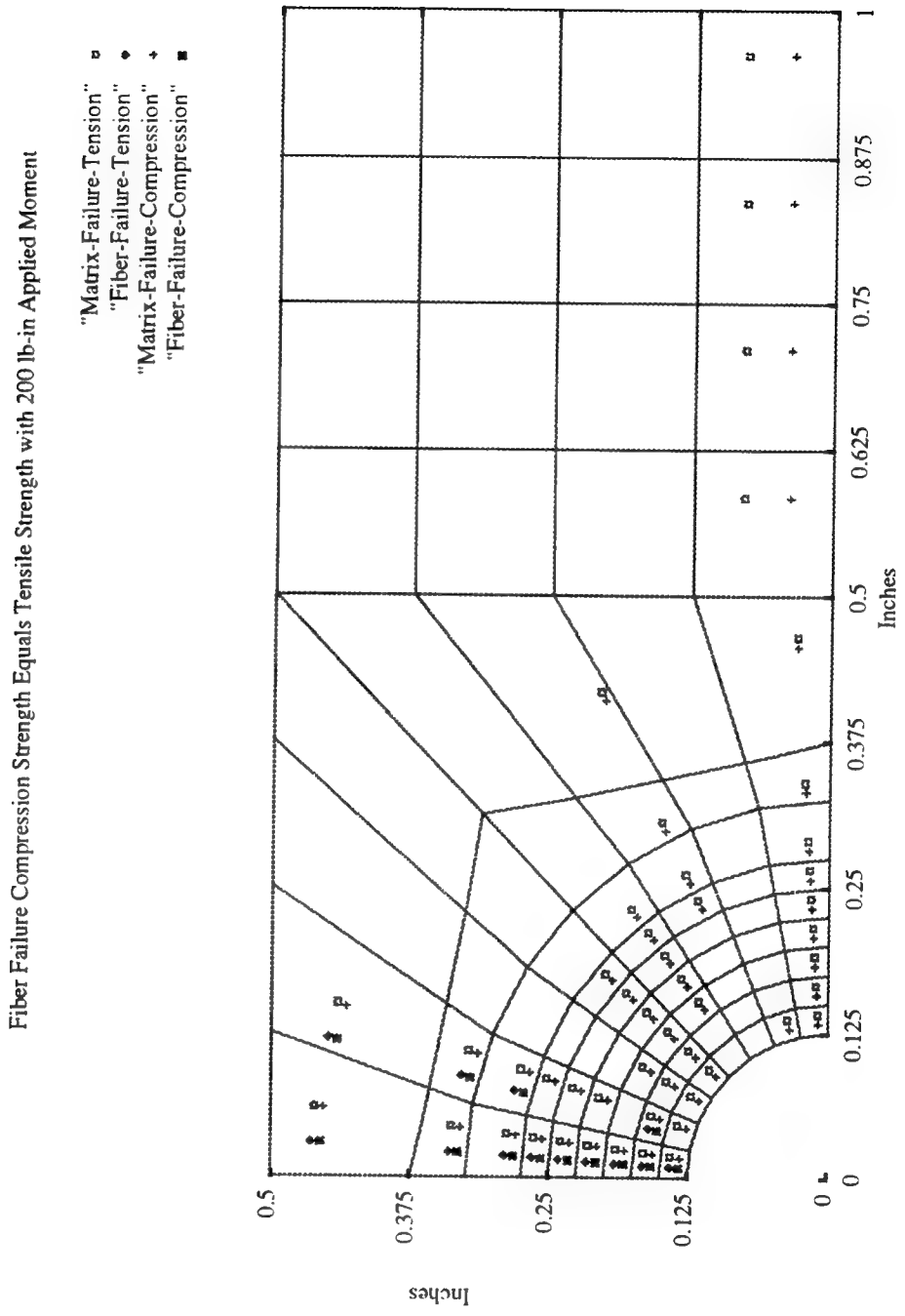

Figure 8. Fiber Failure Compression Strength Equal to Tensile Strength with 200 lb-in Applied Moment

A parametric study was performed by varying the fiber and matrix compressive strengths. The fiber's compressive failure strength was varied while all other composite material properties were held constant as before. The purpose of this study was to determine how the failure load of the composite plate varied in accordance with the change of the compressive strength of the fiber. The matrix compressive strength was then varied while all other material properties of the composite were held constant to analyze its effect on the failure strength of the composite. Figure 9 and Figure 10 show the reduced composite strength for reduced fiber strength and increased matrix strength.

In cases where the fiber compressive failure strength is varied, Figure 9 shows that as the compressive strength of the fiber was decreased, so did the load required to cause failure of the composite. The reduction in the required load is approximately equal to the percent reduction of the compressive failure strength of the fiber. A straight line is drawn in Figure 9 for the cases where both tensile and compressive strengths of the fiber are reduced uniformly. The composite failure load for the reduced fiber's compressive strength only is larger than that for both reduced tensile and compressive strengths of the fiber, as expected. However, there is no more than a 5% difference between the two composite failure loads. As the fiber and compressive strength is reduced more, the composite failure strength deviates further from the straight line because the matrix strength plays a more important role in the composite failure. Although other material properties may influence the finial failure load, the fiber strength is the dominant material property in determining failure load.

Figure 11 through Figure 14 show the damage progression in a composite for various fiber compressive strengths. The results from these figures are used to generate Figure 9. As shown by Figure 11 through Figure 14, the applied moment required for composite failure increases as the fiber compressive strength increases. Composite failure for these cases initiates in the fiber splitting mode in the longitudinal direction and fails in the transverse fiber breakage.

Figure 10 is the graph of resultant failure loads due to changing the matrix's compressive strength while keeping all other composite properties the same as listed in

Table 1. Changing the matrix strength had no effect on the fiber failure load as indicated in Figure 14 through Figure 23 which show the damage progression in a composite with various matrix compressive strengths. Matrix failure occurs at larger bending loads for increased matrix strength as expected. However, the composite failure load changes little for increased matrix strength because the fiber is the dominant material for ultimate failure of the composite structure.

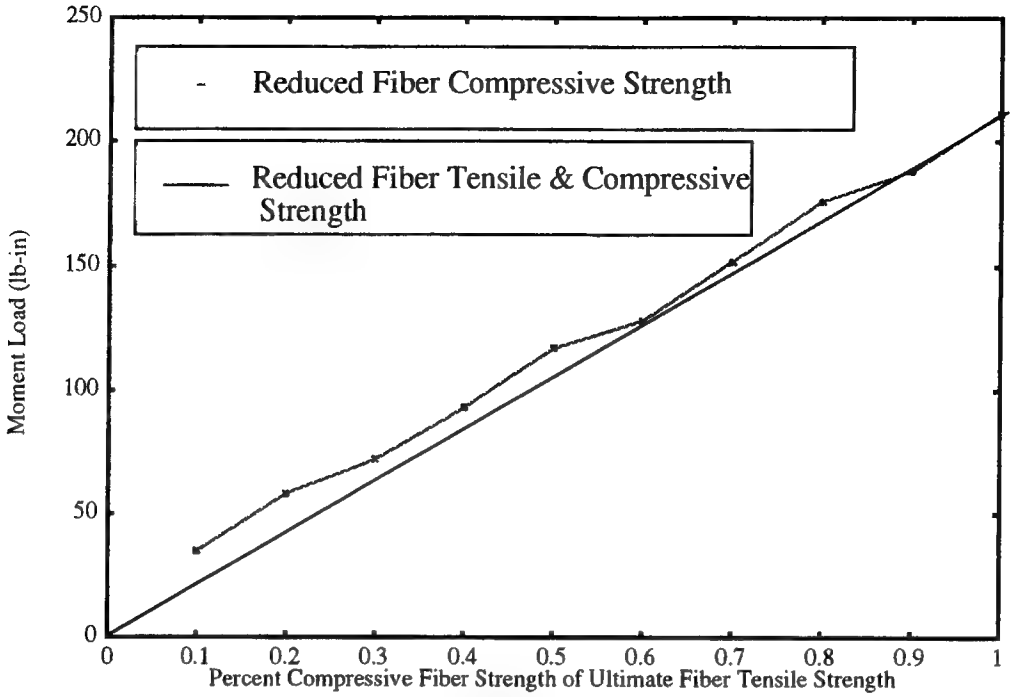

Figure 9. Failure Load with Changing Compressive Fiber Strength

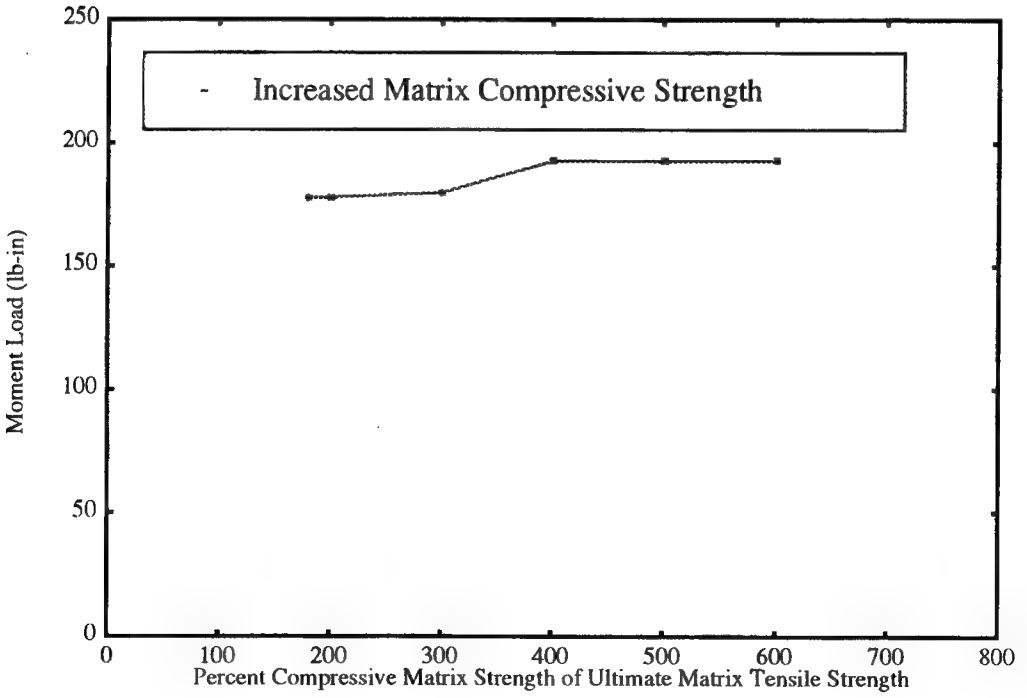

Figure 10. Failure Load with Changing Compressive Matrix Strength

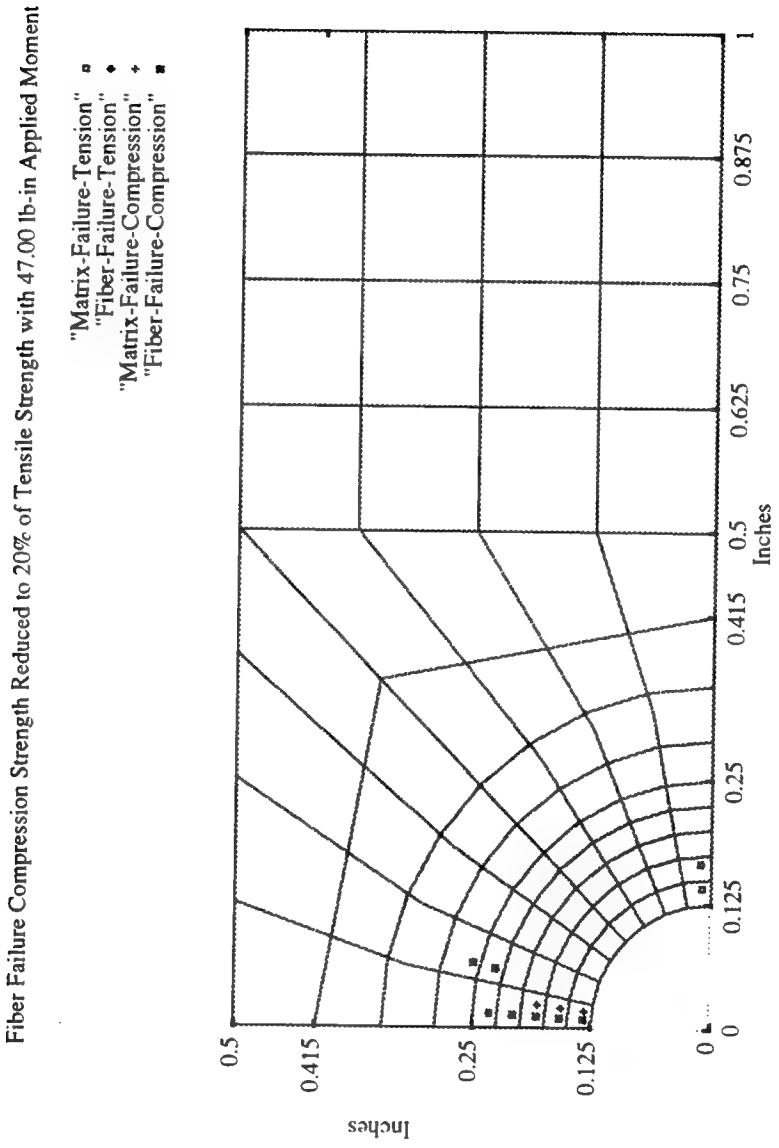

Figure 11. Fiber Failure Compression Strength Reduced to 20% of Tensile Strength with 47.00 lb-in Applied Moment

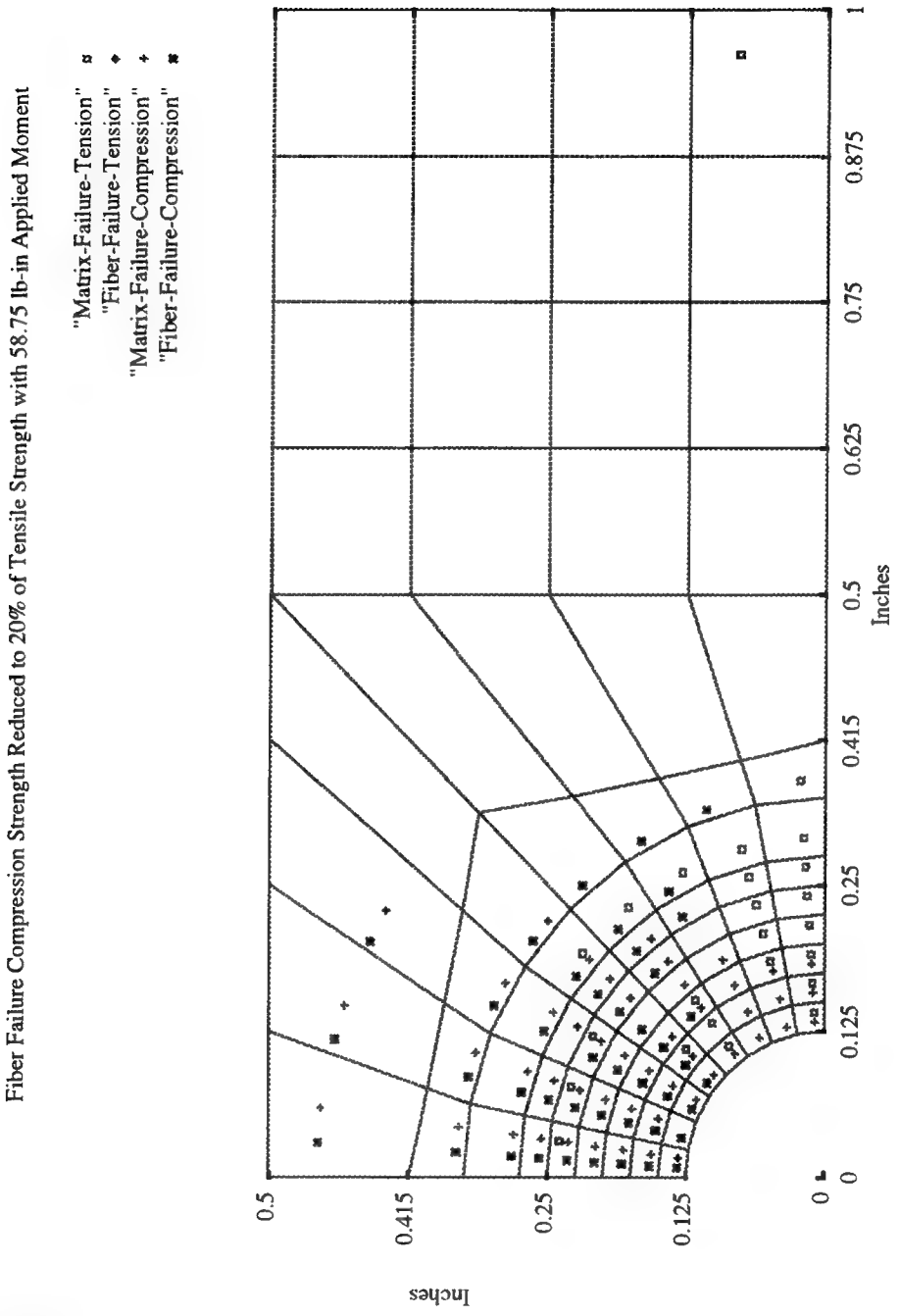

Figure 12. Fiber Failure Compression Strength Reduced to 20% of Tensile Strength with 58.75 lb-in Applied Moment

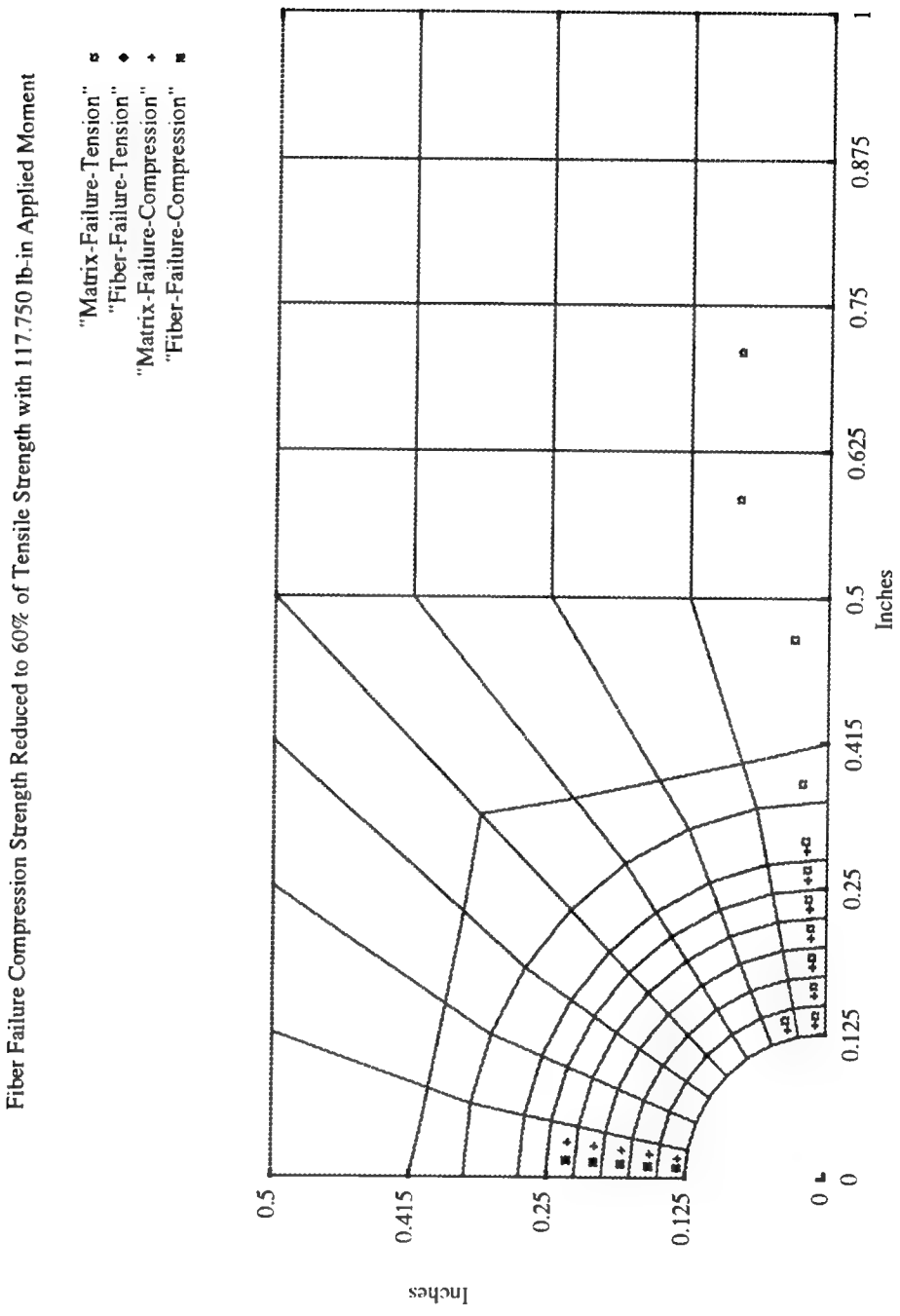

Figure 13. Fiber Failure Compression Strength Reduced to 60% of Tensile Strength with 117.50 lb-in Applied Moment

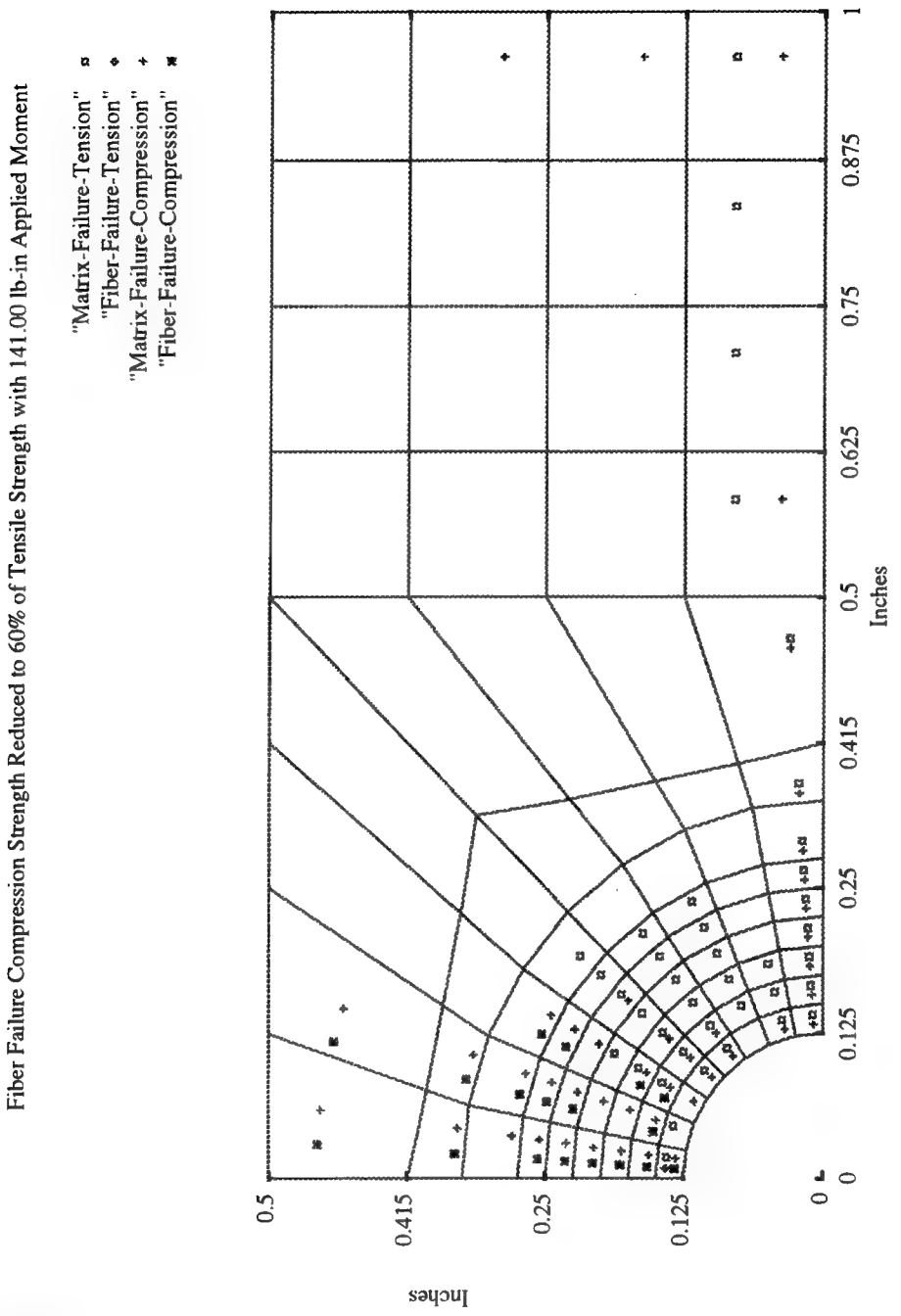

Figure 14. Fiber Failure Compression Strength Reduced to 60% of Tensile Strength with 141.00 lb-in Applied Moment

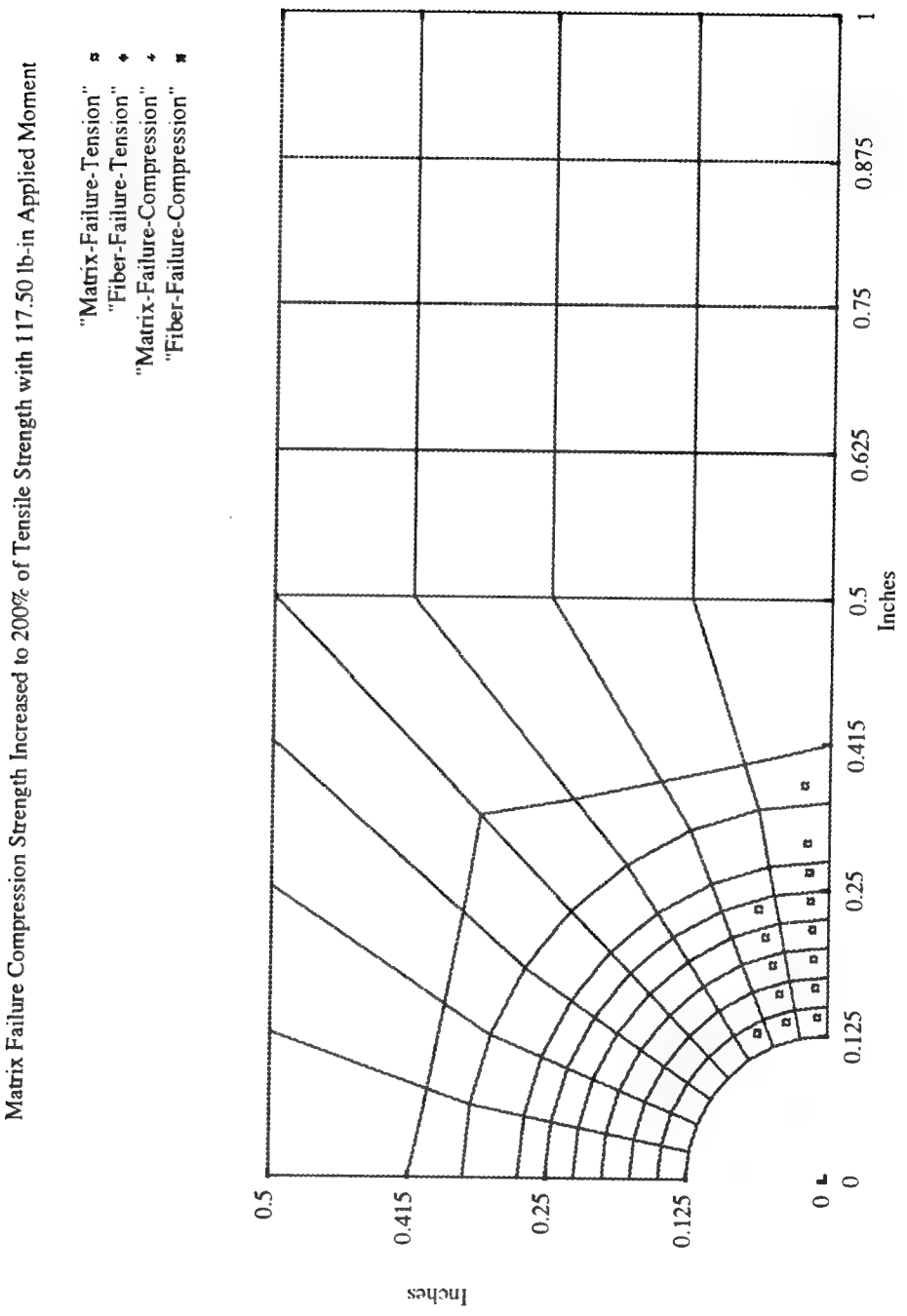

Figure 15. Matrix Failure Compression Strength Increased to 200% of Tensile Strength with 117.50 lb-in Applied Moment

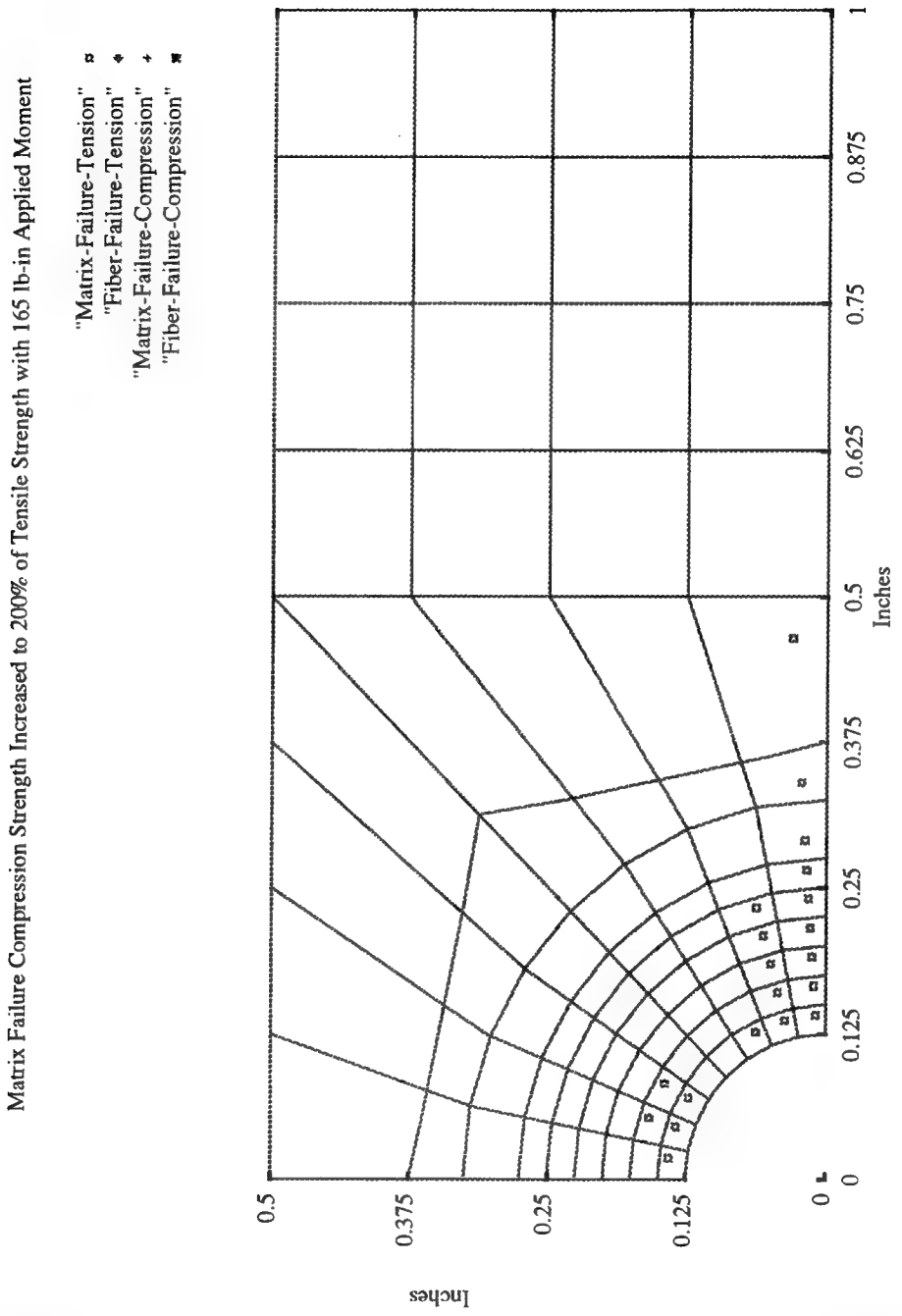

Figure 16. Matrix Failure Compression Strength Increased to 200% of Tensile Strength with 165 lb-in Applied Moment

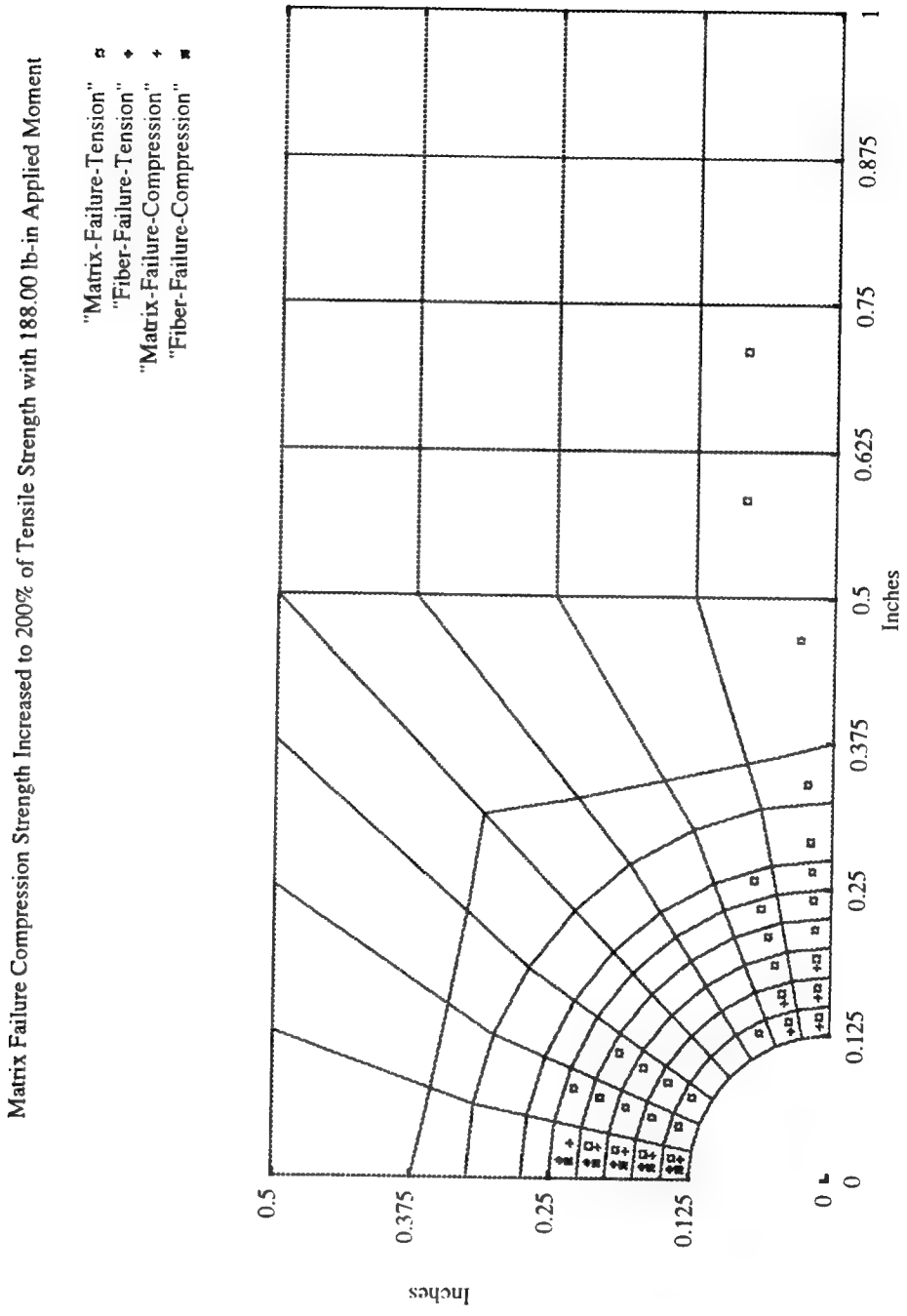

Figure 17. Matrix Failure Compression Strength Increased to 200% of Tensile Strength with 188.00 lb-in Applied Moment

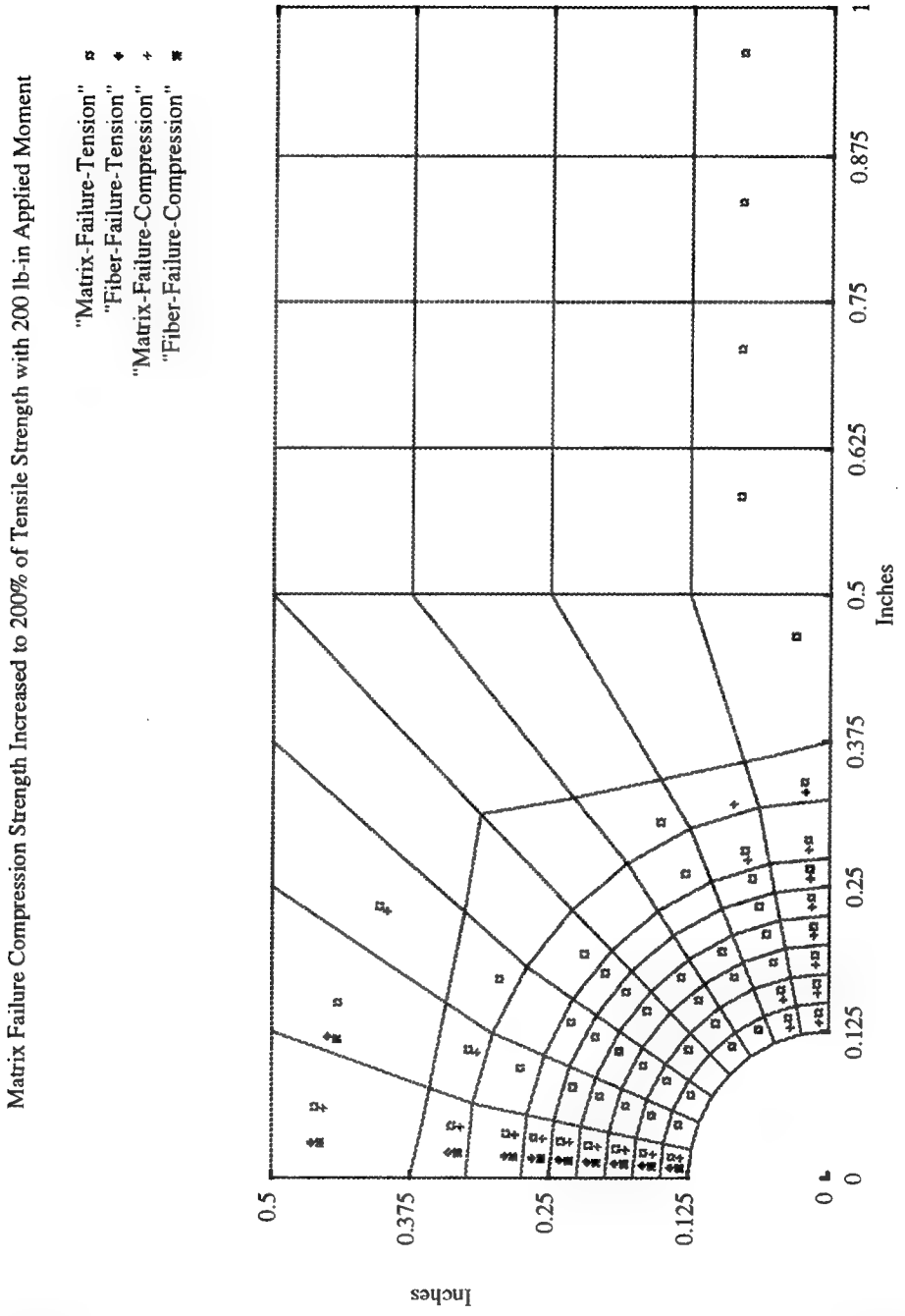

Figure 18. Matrix Failure Compression Strength Increased to 200% of Tensile Strength with 200 lb-in Applied Moment

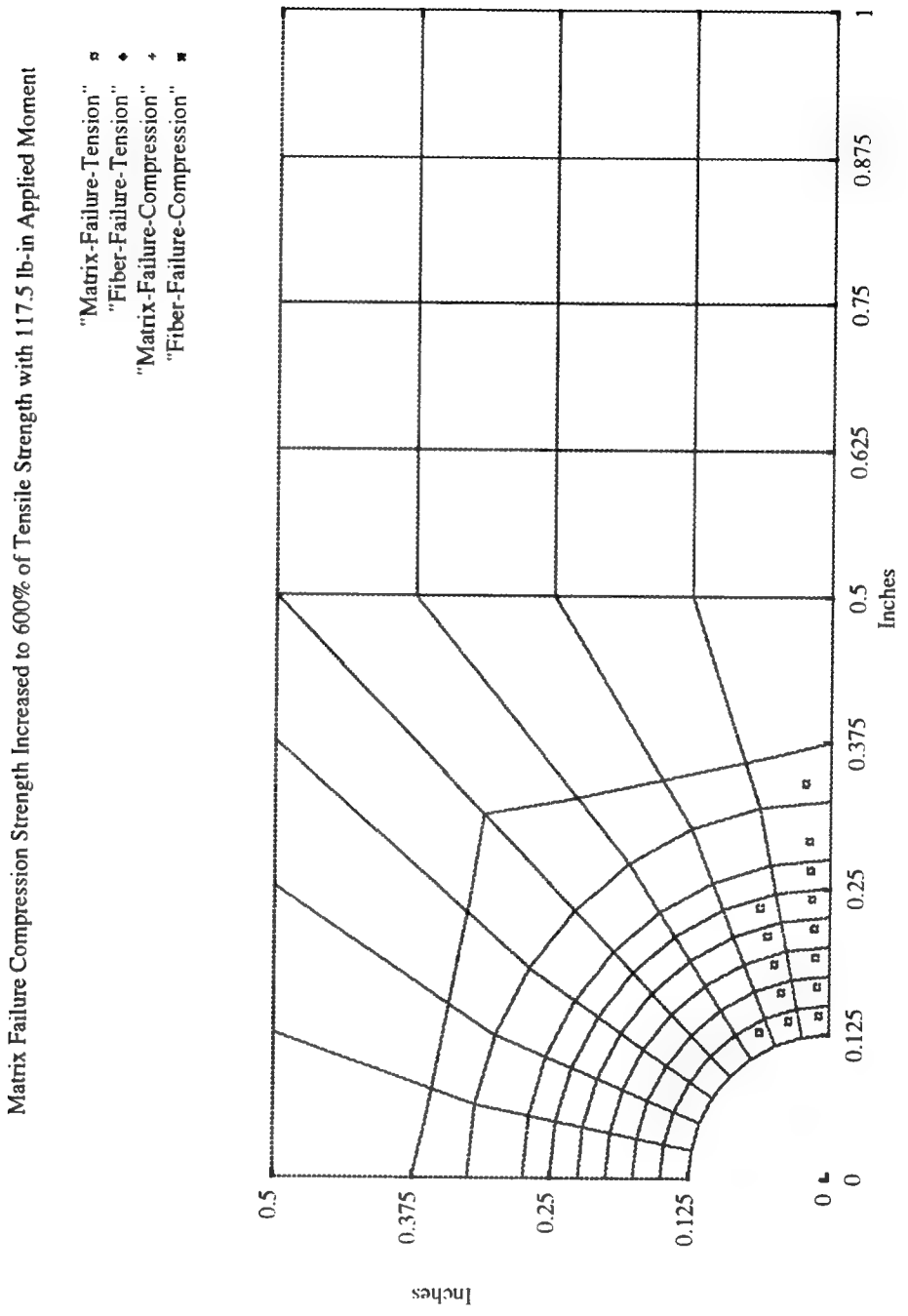

Figure 19. Matrix Failure Compression Strength Increased to 600% of Tensile Strength with 117.50 lb-in Applied Moment

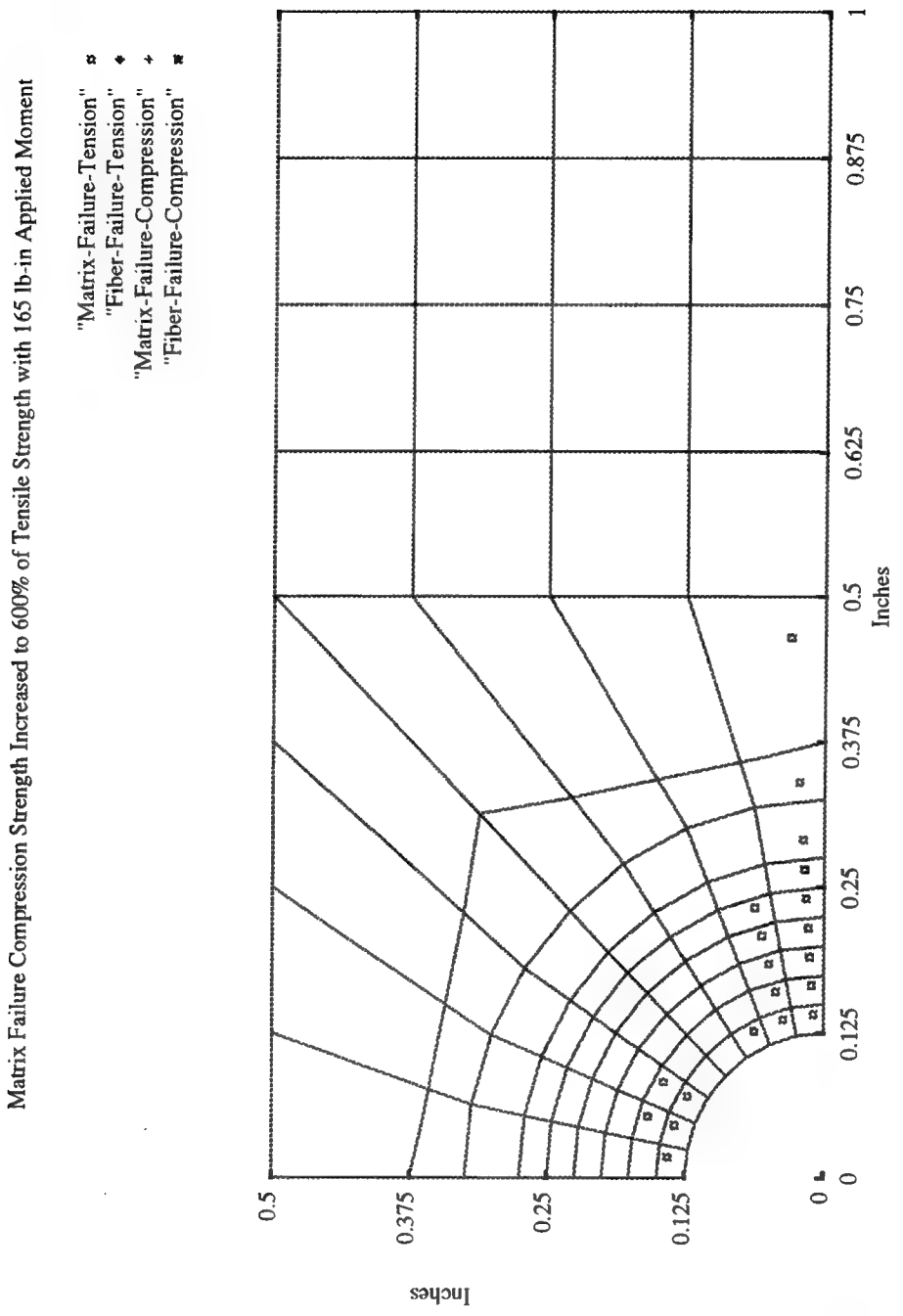

Figure 20. Matrix Failure Compression Strength Equal to 600% of Tensile Strength with 165 lb-in Applied Moment

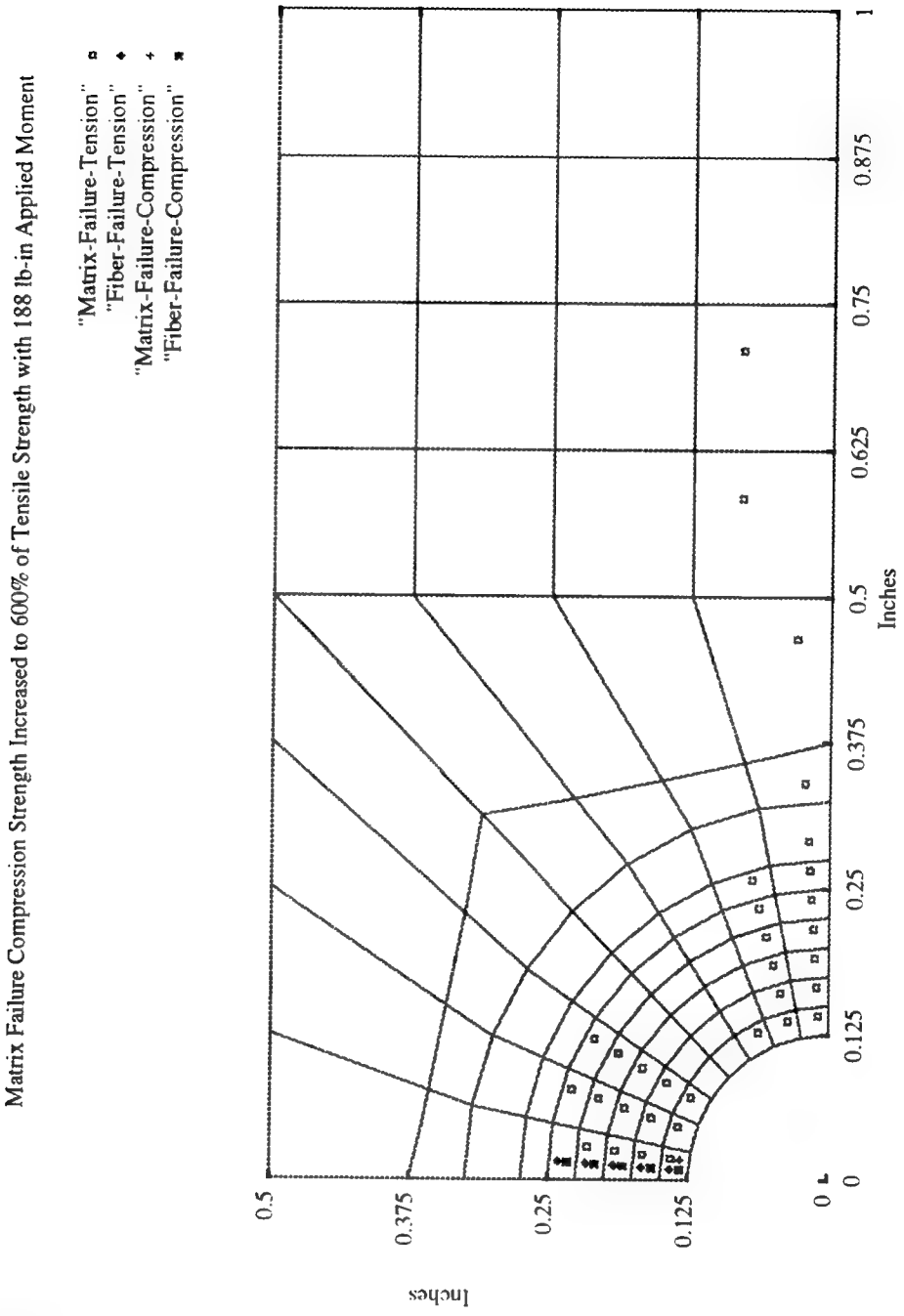

Figure 21. Matrix Failure Compression Strength Increased to 600% of Tensile Strength with 188.00 lb-in Applied Moment

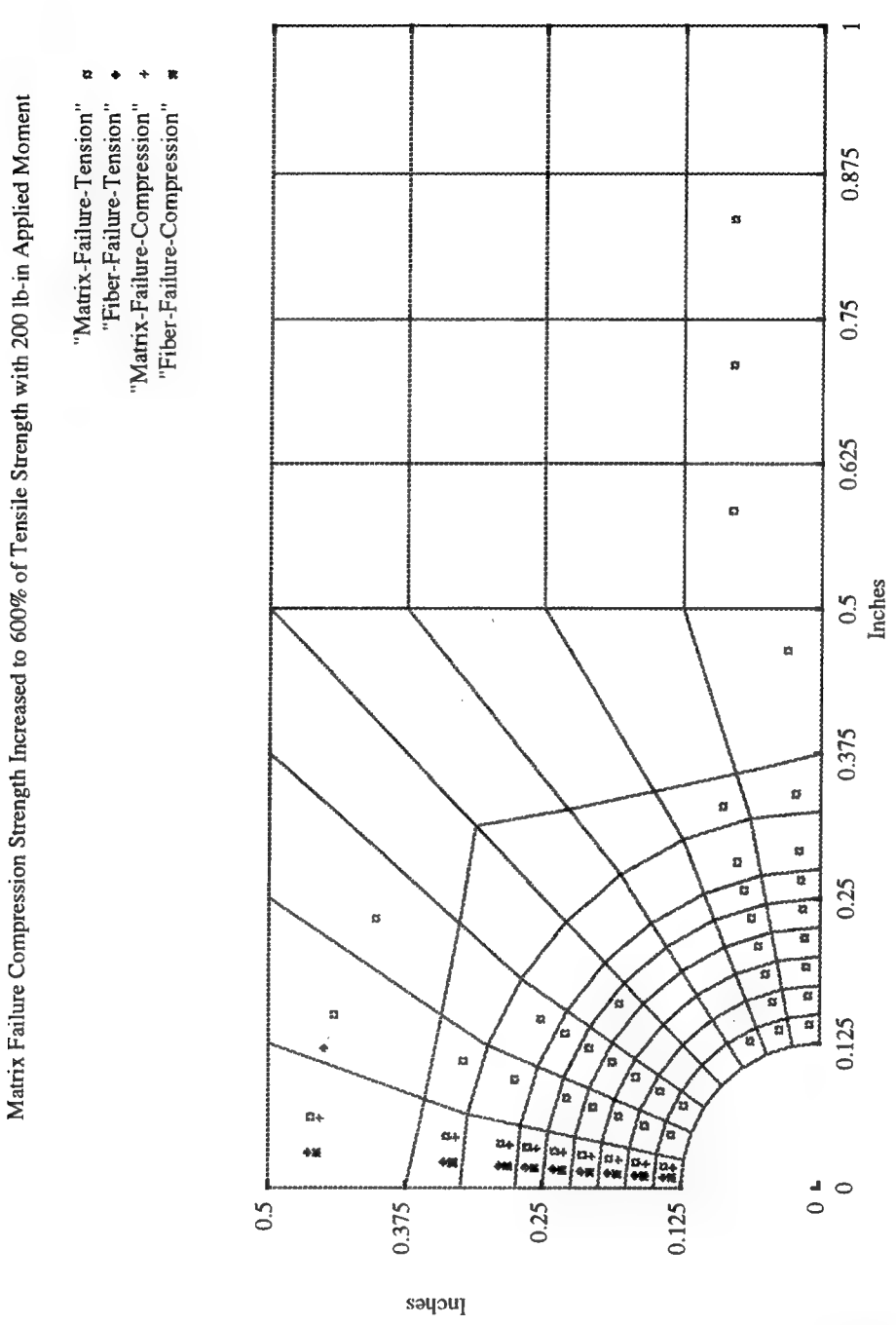

Figure 22. Matrix Failure Compression Strength Increased to 600% of Tensile Strength with 200 lb-in Applied Moment

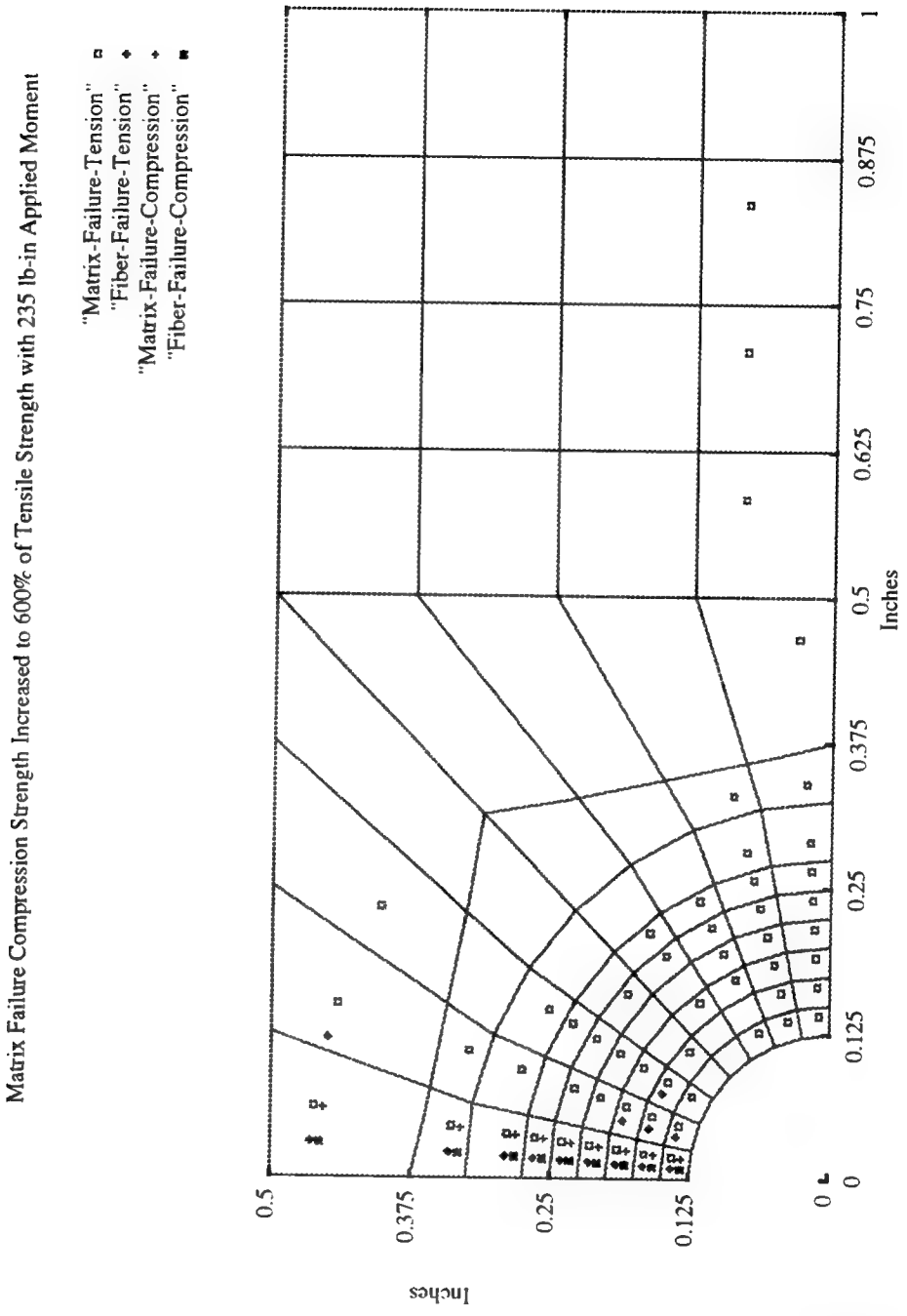

Figure 23. Matrix Failure Compression Strength Increased to 600% of Tensile Strength with 235.00 lb-in Applied Moment

B. SQUARE PLATES SUBJECTED TO TRANSVERSE LOADING

A square plate was used to examine the damage progression that occurs with different boundary and loading conditions. The plate had the length to thickness ratio of 50. A quarter model was used due to plate symmetry. Boundary conditions were either clamped or simply supported on all plate edges. The quarter model would then have adjacent edges clamped or simply supported and the other two adjacent edges symmetric as shown in Figure 24. The applied load was either a concentrated load at the point or a distributed load over the xy plane. Both loads were applied in a positive z direction (into the plane).

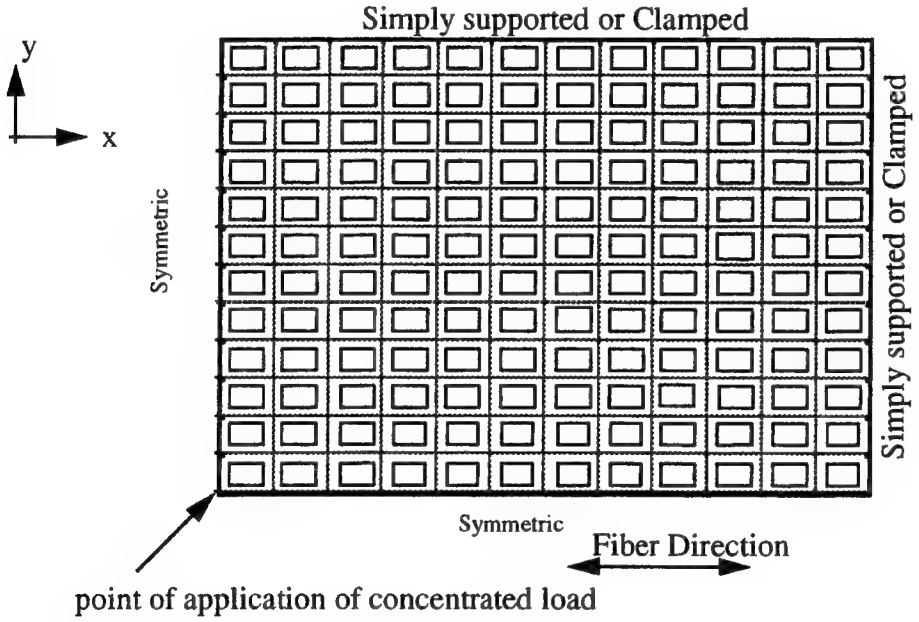

Figure 24. One Quarter Plate Model

Figure 26 through Figure 31 show the resultant damage for each combination of boundary and loading conditions. Under all conditions, the plate could sustain a higher distributed load without failure than a plate with a concentrated load. Complete matrix failure occurs for even a small load for the present composite materials whose properties are the same as those used in the previous section. There is no contribution to composite strength by the present matrix material.

A plate with the clamped boundary condition begins failure along the boundary edge and around the center of the plate. Damage then proceeds between the two as shown in Figure 25 through Figure 28. Simply supported plates show damage initiating around the center of the plate and propagating outward.

The condition of composite failure for this analysis is defined as when the composite is unable to support an applied load and maintain structural integrity. Concentrated loads cause the composite to fail more readily in the clamped condition than in the simply supported condition as indicated by comparing Figure 25 and Figure 26 with Figure 29 and Figure 30.

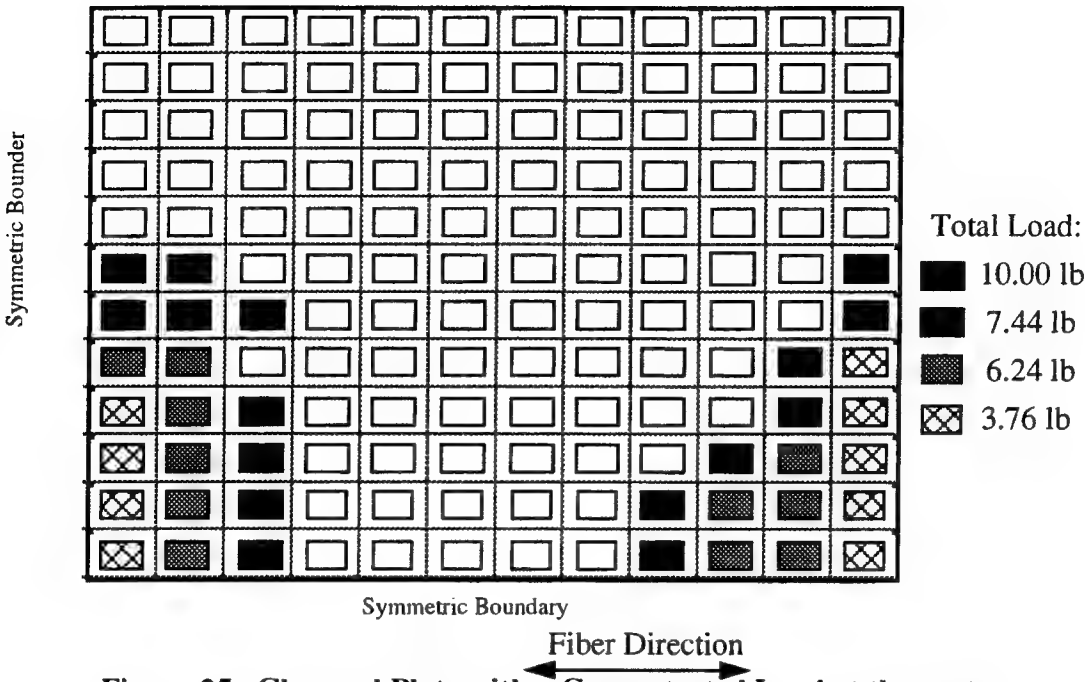

Figure 25. Clamped Plate with a Concentrated Load at the center

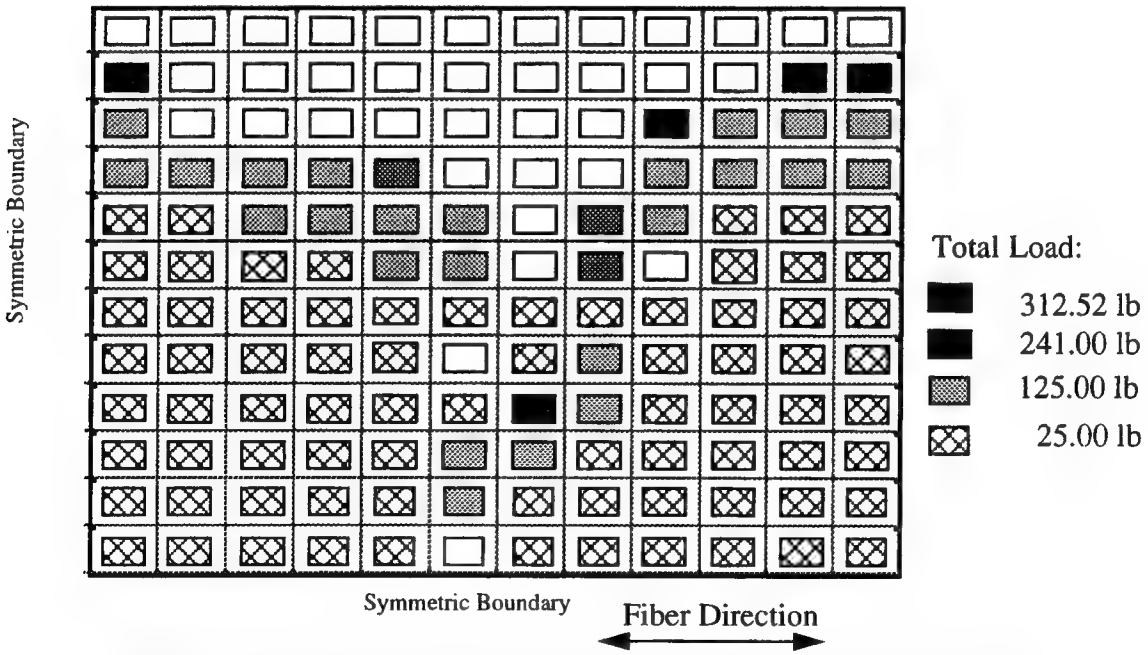

Figure 26. Clamped Plate with a Concentrated Load at the center

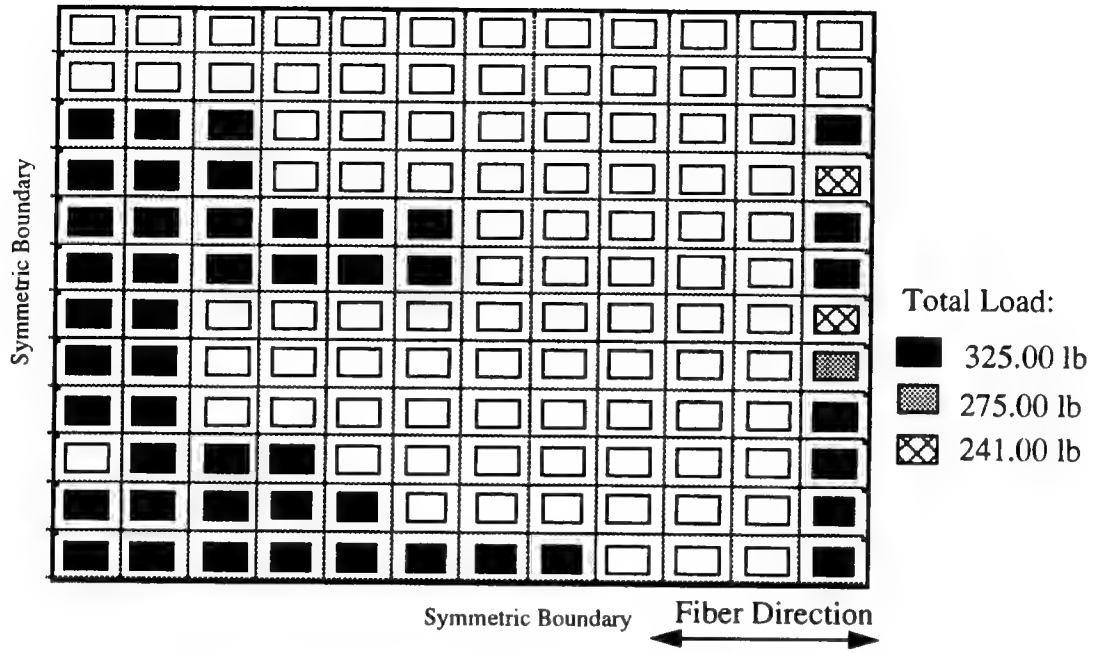

Figure 27. Clamped Plate with a Uniformly Distributed Load

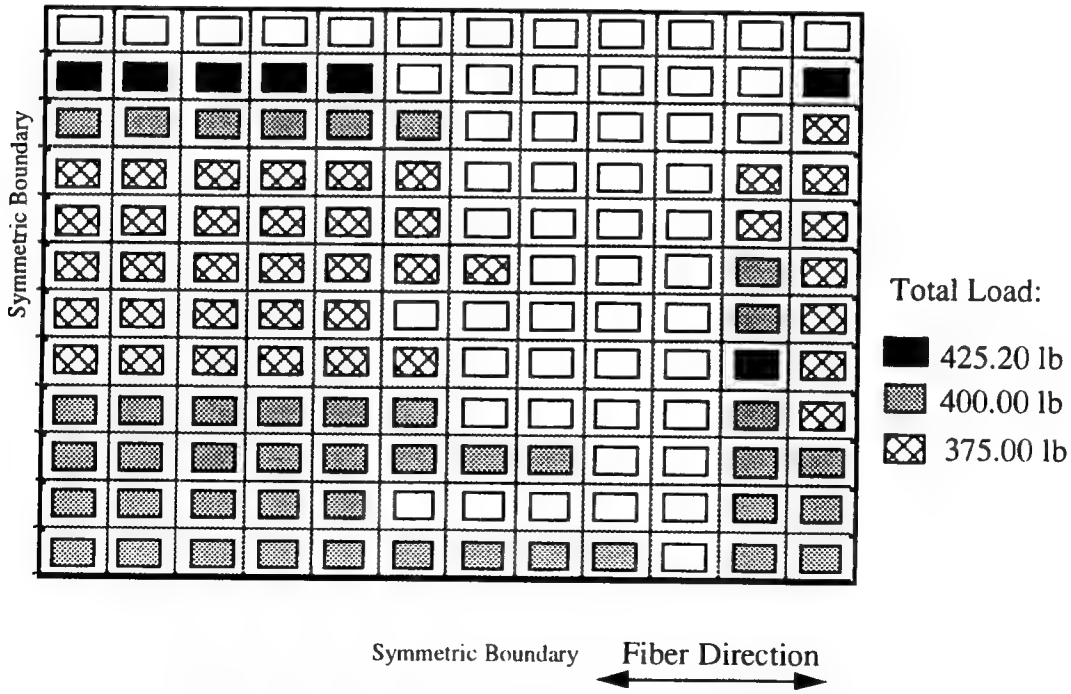

Figure 28. Clamped Plate with a Uniformly Distributed Load

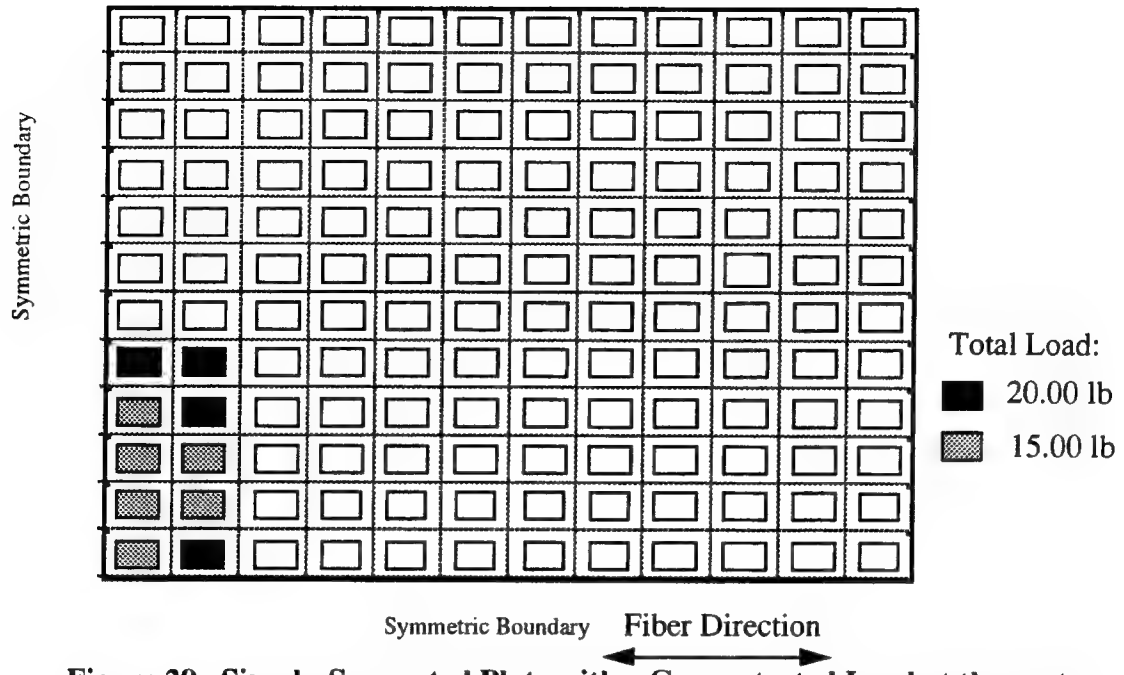

Figure 29. Simply-Supported Plate with a Concentrated Load at the center

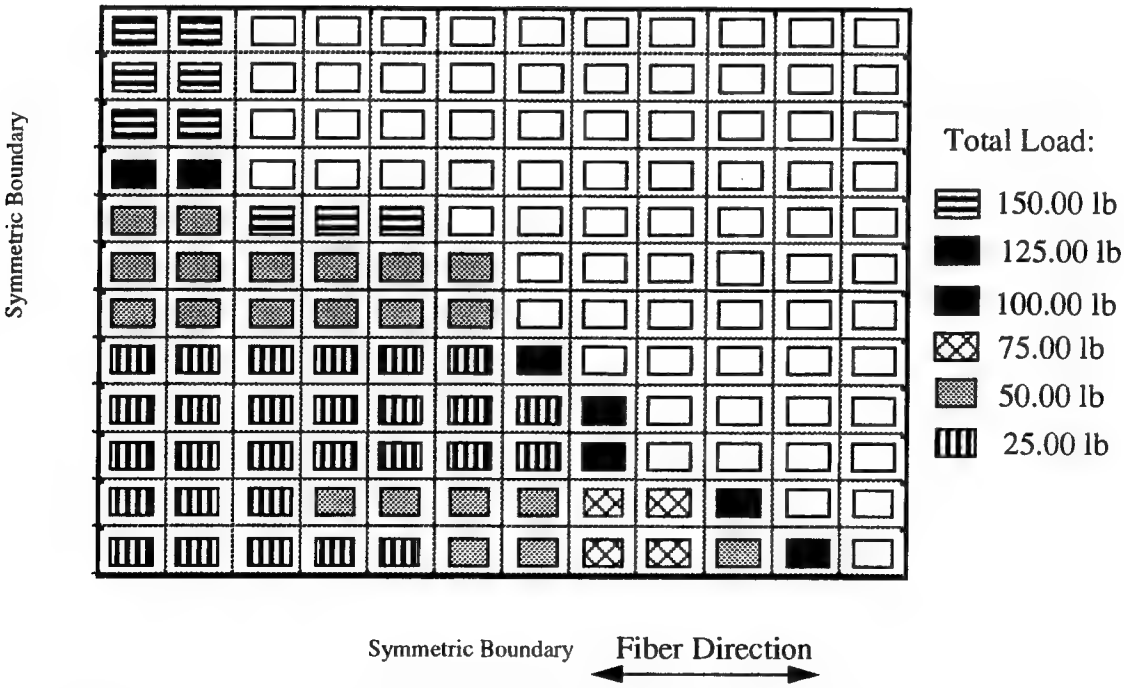

Figure 30. Simply-Supported Plate with a Concentrated Load at the center

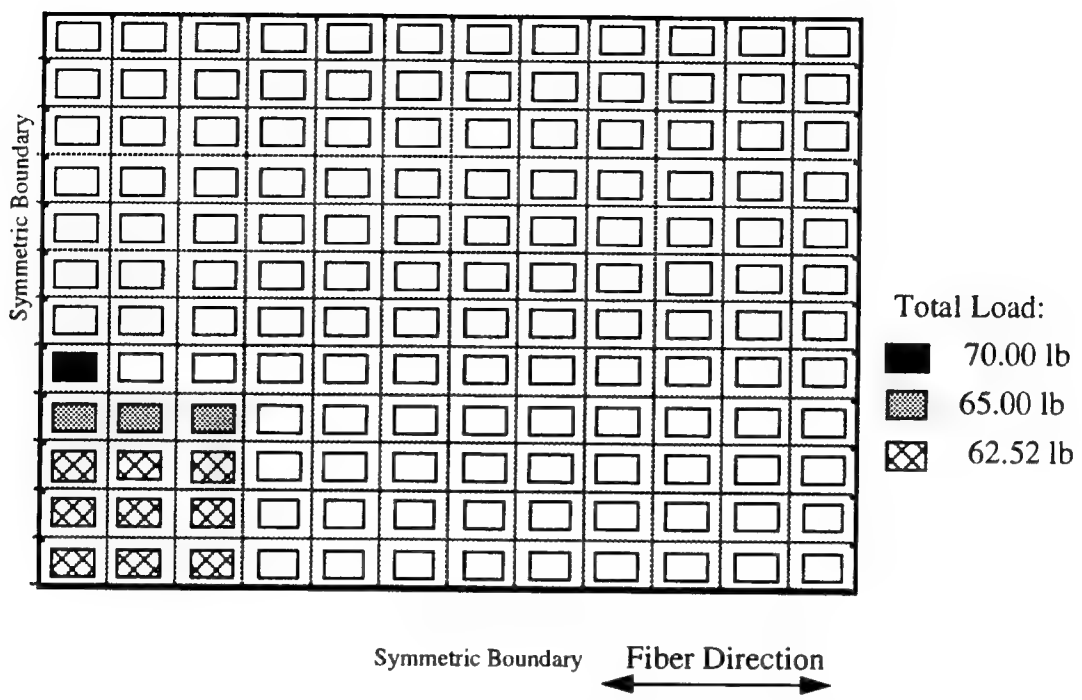

Figure 31. Simply-Supported Plate with a Uniformly Distributed Load

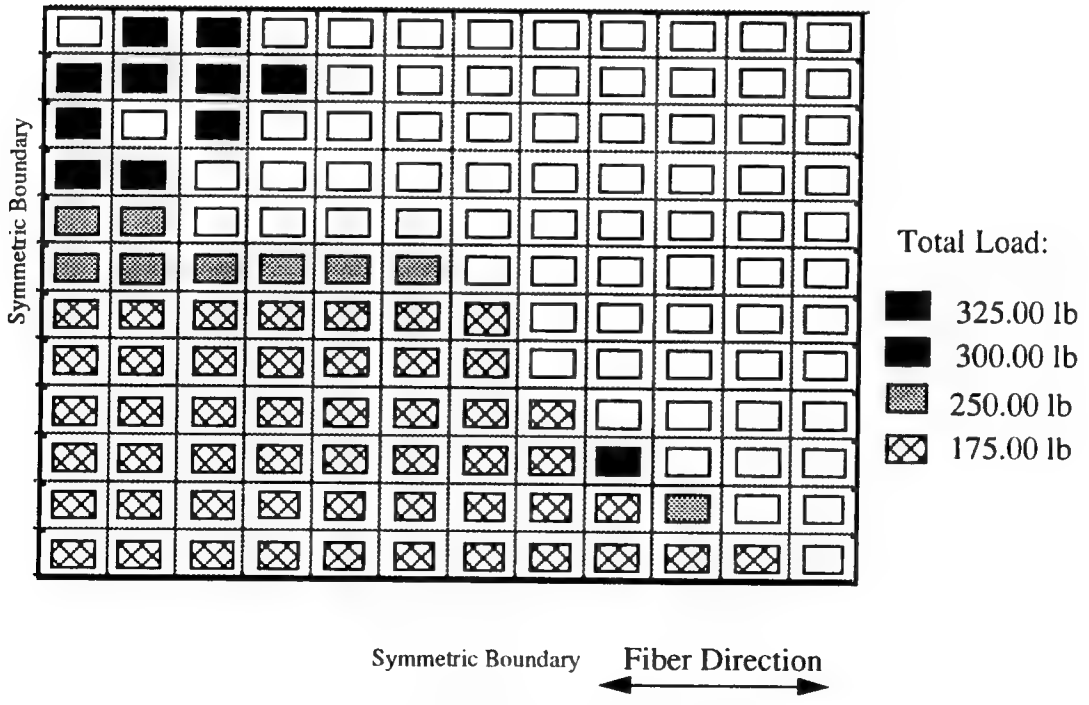

Figure 32. Simply-Supported Plate with Distributed Load

VI. CONCLUSIONS AND RECOMMENDATION

The micro-macromechanical analysis allowed for the study of damage progression in laminated fibrous composites subjected to bending loads. By first applying the micromechanical model developed by Kwon, the composite properties were determined by the material properties of the fiber and matrix. The stresses were determined at the fiber and matrix level by using the micro-macromechanical approach. Failure analysis then could be done based on the stresses in the fiber and matrix. The strength and failure mode of the composite were found from this study. Degradation of failed fiber and matrix material properties was included in the program such that damage propagation could transfer the load from a load from a damaged section to neighboring intact sections resulting increased stresses in the intact area. Applied loads were increased incrementally in the model until complete composite failure occurred.

Good agreement was found between the computer model and experimental results for a carbon/epoxy laminated composite with a circular hole at its center. The parametric study involving the plate clearly showed the dependance of the composite ultimate strength on the fiber strength. As the fiber strength was changed, the composite strength changed in nearly a directly proportional amount.

When the computer model was used to study a square plate with transverse loading, the failure pattern was as expected for such conditions. The square plate study also showed that a greater load could be maintained on the plate with less damage when a uniformly distributed load was applied instead of a concentrated load.

It is suggested that this study be extend to cover cases involving multiple holes to determine how their proximity to each other in a plate influences damage progression. More experimental results need to be obtained to further verify the damage model.

APPENDIX: FINITE ELEMENT MATRICES

$$[\delta]_e = \begin{bmatrix} u_1^b \\ v_1^b \\ u_1^t \\ v_1^t \\ w_1 \\ u_2^b \\ v_2^b \\ u_2^t \\ v_2^t \\ w_2 \\ u_3^b \\ v_3^b \\ u_3^t \\ v_3^t \\ w_3 \\ u_4^b \\ v_4^b \\ u_4^t \\ v_4^t \\ w_4 \end{bmatrix}$$

$$
\begin{Bmatrix} \varepsilon_x \\ \varepsilon_y \\ \varepsilon_z \\ \gamma_{xy} \\ \gamma_{yz} \\ \gamma_{zx} \end{Bmatrix}
=
\begin{bmatrix}
\frac{\partial \overline{N}_1}{\partial x} & 0 & 0 & \frac{\partial \overline{N}_2}{\partial x} & 0 & 0 & \frac{\partial \overline{N}_3}{\partial x} & 0 & 0 & \frac{\partial \overline{N}_4}{\partial x} & 0 & 0 & \frac{\partial \overline{N}_5}{\partial x} & 0 & 0 & \frac{\partial \overline{N}_6}{\partial x} & 0 & 0 & \frac{\partial \overline{N}_7}{\partial x} & 0 & 0 & \frac{\partial \overline{N}_8}{\partial x} & 0 & 0 \\
0 & \frac{\partial \overline{N}_1}{\partial y} & 0 & 0 & \frac{\partial \overline{N}_2}{\partial y} & 0 & 0 & \frac{\partial \overline{N}_3}{\partial y} & 0 & 0 & \frac{\partial \overline{N}_4}{\partial y} & 0 & 0 & \frac{\partial \overline{N}_5}{\partial y} & 0 & 0 & \frac{\partial \overline{N}_6}{\partial y} & 0 & 0 & \frac{\partial \overline{N}_7}{\partial y} & 0 & 0 & \frac{\partial \overline{N}_8}{\partial y} & 0 \\
0 & 0 & \frac{\partial \overline{N}_1}{\partial z} & 0 & 0 & \frac{\partial \overline{N}_2}{\partial z} & 0 & 0 & \frac{\partial \overline{N}_3}{\partial z} & 0 & 0 & \frac{\partial \overline{N}_4}{\partial z} & 0 & 0 & \frac{\partial \overline{N}_5}{\partial z} & 0 & 0 & \frac{\partial \overline{N}_6}{\partial z} & 0 & 0 & \frac{\partial \overline{N}_7}{\partial z} & 0 & 0 & \frac{\partial \overline{N}_8}{\partial z} \\
\frac{\partial \overline{N}_1}{\partial y} & \frac{\partial \overline{N}_1}{\partial x} & 0 & \frac{\partial \overline{N}_2}{\partial y} & \frac{\partial \overline{N}_2}{\partial x} & 0 & \frac{\partial \overline{N}_3}{\partial y} & \frac{\partial \overline{N}_3}{\partial x} & 0 & \frac{\partial \overline{N}_4}{\partial y} & \frac{\partial \overline{N}_4}{\partial x} & 0 & \frac{\partial \overline{N}_5}{\partial y} & \frac{\partial \overline{N}_5}{\partial x} & 0 & \frac{\partial \overline{N}_6}{\partial y} & \frac{\partial \overline{N}_6}{\partial x} & 0 & \frac{\partial \overline{N}_7}{\partial y} & \frac{\partial \overline{N}_7}{\partial x} & 0 & \frac{\partial \overline{N}_8}{\partial y} & \frac{\partial \overline{N}_8}{\partial x} & 0 \\
0 & \frac{\partial \overline{N}_1}{\partial z} & \frac{\partial \overline{N}_1}{\partial y} & 0 & \frac{\partial \overline{N}_2}{\partial z} & \frac{\partial \overline{N}_2}{\partial y} & 0 & \frac{\partial \overline{N}_3}{\partial z} & \frac{\partial \overline{N}_3}{\partial y} & 0 & \frac{\partial \overline{N}_4}{\partial z} & \frac{\partial \overline{N}_4}{\partial y} & 0 & \frac{\partial \overline{N}_5}{\partial z} & \frac{\partial \overline{N}_5}{\partial y} & 0 & \frac{\partial \overline{N}_6}{\partial z} & \frac{\partial \overline{N}_6}{\partial y} & 0 & \frac{\partial \overline{N}_7}{\partial z} & \frac{\partial \overline{N}_7}{\partial y} & 0 & \frac{\partial \overline{N}_8}{\partial z} & \frac{\partial \overline{N}_8}{\partial y} \\
\frac{\partial \overline{N}_1}{\partial z} & 0 & \frac{\partial \overline{N}_1}{\partial x} & \frac{\partial \overline{N}_2}{\partial z} & 0 & \frac{\partial \overline{N}_2}{\partial x} & \frac{\partial \overline{N}_3}{\partial z} & 0 & \frac{\partial \overline{N}_3}{\partial x} & \frac{\partial \overline{N}_4}{\partial z} & 0 & \frac{\partial \overline{N}_4}{\partial x} & \frac{\partial \overline{N}_5}{\partial z} & 0 & \frac{\partial \overline{N}_5}{\partial x} & \frac{\partial \overline{N}_6}{\partial z} & 0 & \frac{\partial \overline{N}_6}{\partial x} & \frac{\partial \overline{N}_7}{\partial z} & 0 & \frac{\partial \overline{N}_7}{\partial x} & \frac{\partial \overline{N}_8}{\partial z} & 0 & \frac{\partial \overline{N}_8}{\partial x} \\
0 & \frac{\partial \overline{N}_1}{\partial z} & \frac{\partial \overline{N}_1}{\partial y} & 0 & \frac{\partial \overline{N}_2}{\partial z} & \frac{\partial \overline{N}_2}{\partial y} & 0 & \frac{\partial \overline{N}_3}{\partial z} & \frac{\partial \overline{N}_3}{\partial y} & 0 & \frac{\partial \overline{N}_4}{\partial z} & \frac{\partial \overline{N}_4}{\partial y} & 0 & \frac{\partial \overline{N}_5}{\partial z} & \frac{\partial \overline{N}_5}{\partial y} & 0 & \frac{\partial \overline{N}_6}{\partial z} & \frac{\partial \overline{N}_6}{\partial y} & 0 & \frac{\partial \overline{N}_7}{\partial z} & \frac{\partial \overline{N}_7}{\partial y} & 0 & \frac{\partial \overline{N}_8}{\partial z} & \frac{\partial \overline{N}_8}{\partial y} & \frac{\partial N_4}{\partial x} \\
\frac{\partial \overline{N}_1}{\partial z} & \frac{\partial \overline{N}_1}{\partial y} & \frac{\partial \overline{N}_1}{\partial x} & \frac{\partial \overline{N}_2}{\partial z} & \frac{\partial \overline{N}_2}{\partial y} & \frac{\partial N_1}{\partial x} & \frac{\partial \overline{N}_3}{\partial z} & \frac{\partial \overline{N}_3}{\partial y} & \frac{\partial N_2}{\partial x} & \frac{\partial \overline{N}_4}{\partial z} & \frac{\partial \overline{N}_4}{\partial y} & \frac{\partial N_2}{\partial x} & \frac{\partial \overline{N}_5}{\partial z} & \frac{\partial \overline{N}_5}{\partial y} & \frac{\partial N_3}{\partial x} & \frac{\partial \overline{N}_6}{\partial z} & \frac{\partial \overline{N}_6}{\partial y} & \frac{\partial N_3}{\partial x} & \frac{\partial \overline{N}_7}{\partial z} & \frac{\partial \overline{N}_7}{\partial y} & \frac{\partial N_4}{\partial x} & \frac{\partial \overline{N}_8}{\partial z} & \frac{\partial \overline{N}_8}{\partial y} & \frac{\partial N_4}{\partial x}
\end{bmatrix}
\cdot
\begin{bmatrix}
u_1^b \\ v_1^b \\ u_1^r \\ v_1^r \\ w_1 \\ u_2^b \\ v_2^b \\ u_2^r \\ v_2^r \\ w_2 \\ u_3^b \\ v_3^b \\ u_3^r \\ v_3^r \\ w_3 \\ u_4^b \\ v_4^b \\ u_4^r \\ v_4^r \\ w_4
\end{bmatrix}
$$

LIST OF REFERENCES

Berner, J. M., *Finite Element Analysis of Damage in Fibrous Composities Using A Micromechanical Model,* Master's Thesis, Naval Postgraduate School, Monterey, California, December 1993.

Chang, F. K., Chang, K.Y., "A Progressive Damage Model for Laminated Composites Containing Stess Concentrations", *Journal of Composite Materials,* vol. 21, pp.834-855, 1987.

Kwon, Y. W., "Finite Element Analysis of Crack Closure in Plate Bending", *Composites & Structures,* vol. 32, no.6, pp. 1439-1445, 1988.

Kwon, Y. W., "Calculation of Effective Moduli of Fibrous Composites with Micro-Mechanical Damage", *Composite Structures,* vol. 25, pp 187-192, 1993.

Kwon, Y. W., Salinas, D., Neibert, M., J., "Thermally Induced Stresses in a Trilayered System", *Journal of Thermal Stresses*, vol. 17, pp. 491-508, 1994.

Kwon, Y. W., "Symmetric Conditions of Plates", unpublished notes presented in a private lecture, Naval Postgraudate School, March 1994.

Owen, D. R. J., Li, Z. H., "A Refined Analysis of Laminated Plates by Finite Element Displacement Methods-I. Fundamentals and Static Analysis", *Composites & Structures,* vol. 26, no. 6, pp. 907-914, 1987

Segerlind, L. J., *Applied Finite Element Analysis*, John Wiley and Sons, New York, New York, 1984.

Ugural, A. C., Fenster S. K., *Advanced Strength and Applied Elasticity,* P T R Prentice-Hall, Inc., Englewood Cliffs, New Jersey, 1987.

Yamada, S. E., Sun, C. T., Analysis of Laminated Strength and Its Distribution, *Journal of Composite Materials,* vol. 12, pp. 275-284, 1978

Yang, S. T., *Study of Failure in Fibrous Composites Subjected to Bending Loads,* Master's Thesis, Naval Postgraduate School, Monterey, California, June 1994.

INITIAL DISTRIBUTION LIST

1.	Defense Technical Information Center Cameron Station Alexandria, VA 22304-6145	2
2.	Dudley Knox Library Code 052 Naval Postgraduate School Monterey, CA 93943-5002	2
3.	Chairman, Code 34 NE Department of Mechanical Engineering Naval Postgraduate School Monterey, CA 93943-5000	1
4.	Professor Y. W. Kwon, Code ME/Kw Department of Mechanical Engineering Naval Postgraduate School Monterey, CA 93943-5000	2
5.	Dr. Shaio-Wen Wang Advanced Metallic & Cermic Branch (6063) Aircraft Division Naval Air Warfare Center Warminster, PA 18974-0591	1
6.	Dr. Roland Cochran Polymer Composite Center Aircraft Division Naval Air Warfare Center Warminster, PA 18974-0591	1
7.	Mr. David Bonnani Naval Surface Warfare Center, Carderock Div. Code 1720.2 Bethesda, MD 20084-5000	1
8.	Mr. Erik A. Rasmussen Naval Surface Warfare Center, Carderock Div. Code 332 800 North Quincy Street Arlington, VA 22217-5000	1

9. Dr. Phillip B. Abraham 1
Office of Naval Research Mechanics Div.
Code 332
800 North Quincy Street
Arlington, VA 22217-5000

10. LT Bruce H. Hamilton 1
4408 Parview Drive
Charlotte, NC 28226